UNIVERSITÀ DI PISA

Electromagnetic Radiations and Biological Interactions

"Laurea Magistrale" in Biomedical Engineering
First semester (6 credits, 60 hours), academic year 2011/12

Prof. Paolo Nepa
p.nepa@iet.unipi.it

Non Ionizing Radiation (NIR) Dosimetry

Edited by Dr. Anda Guraliuc

MRL Microwave & Radiation Laboratory

Lecture Content

- **Dosimetric parameters**
- **Analytical dosimetry**
  - Homogenous sphere
  - Prolate homogenous spheroid
  - Homogenous ellipsoid
  - Infinite cylinder
- **Numerical dosimetry**
- **Examples**

Introduction

- The electromagnetic environment consists of **natural radiation and man-made electromagnetic fields**, the latter are produced either intentionally or as by-products of the use of electrical devices and systems.

- The **natural electromagnetic environment** originates from terrestrial and electrical discharges in the earth's atmosphere and wide spectrum radiation from sun and space.

- The everyday use of devices and systems emitting electromagnetic fields is continuously increasing. The *man-made electromagnetic environment* also comes from cellular mobile communication networks, wireless handsets and cell phones etc.

- Sources generating high levels of electromagnetic fields are typically found in medical applications (magnetic resonance imaging, diathermy, hyperthermia, various kinds of RF ablation) and at certain workplaces (welding machines, RF/microwave heating equipment, long-range radars).

Dosimetry plays an important role in risk evaluation of human exposure to NIR as it quantifies the interaction of non-ionizing radiations with biological tissues.

NIR Dosimetry

➢ Dosimetry consists in:

• quantification of the absorbed power of a human body exposed to an electromagnetic field
• determination of absorbed power distribution

➢ **Numerical approach**: development of analytical and numerical (or hybrid analytical-numerical) simplified models and implementation of computer codes for numerical calculations.

➢ **Experimental approach**: measurements on phantoms or animals.

Exposure levels in the microwave range are usually described in terms of power density, W/m^2, associated to an incident plane wave. However, close to RF sources with longer wavelength, the values of both the electric and magnetic field strengths are needed to describe the field source.

NIR Dosimetry and SAR

Three different quantities are commonly used in dosimetry:

✓ at low frequencies (below 100 kHz), many biological effects are quantified in terms of the **current density**.

✓ at higher frequencies, many (but not all) interactions are due to **the rate of energy deposition per unit mass**: the **specific absorption rate (SAR, W/Kg)** is used as the dosimetric parameter.

✓ At frequencies higher than tens of GHz interactions are limited to the body surface, and **the rate of energy deposition per unit surface** is often considered.

Specific Absorption Rate (SAR)

Problem: a biological material, non homogeneous, of a mass M and volume V. What is the EM power dissipated into the material when the latter is exposed to an electromagnetic field characterized by a certain power density, polarization, frequency, etc ?

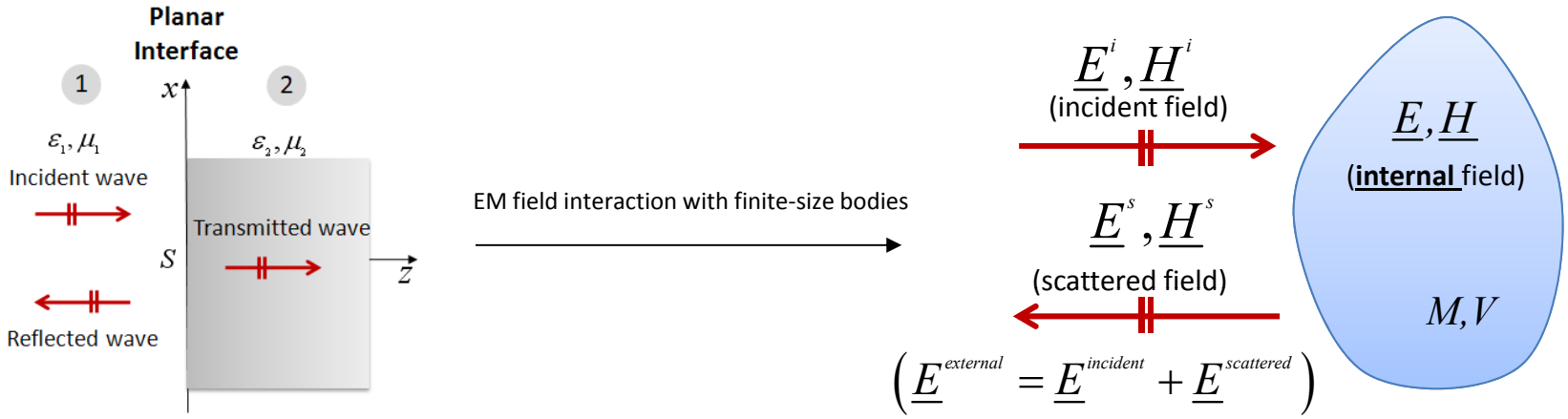

$$SAR(\underline{r}) = \frac{\sigma(\underline{r})\left|\underline{E}(\underline{r})\right|^2}{2\rho(\underline{r})} \quad [\text{W/kg}]$$

Specific Absorption Rate (local SAR)

$\underline{E}$ - the electric field **inside** the volume V: **INTERNAL FIELD** [V/m] ρ - material density [kg/m^3]

σ - material conductivity [S/m]

$$\left(SAR(\underline{r}) = \frac{\left(\frac{1}{2}\sigma(\underline{r})\left|\underline{E}(\underline{r})\right|^2 dV\right)}{\rho(\underline{r})dV} \right) \qquad \left(\tilde{\varepsilon} = \varepsilon' - j\varepsilon'' = \varepsilon' - j\frac{\sigma}{\omega\varepsilon_0} \right)$$

SAR VISUALIZATION

2D or 3D plot including information about position of local hot spots

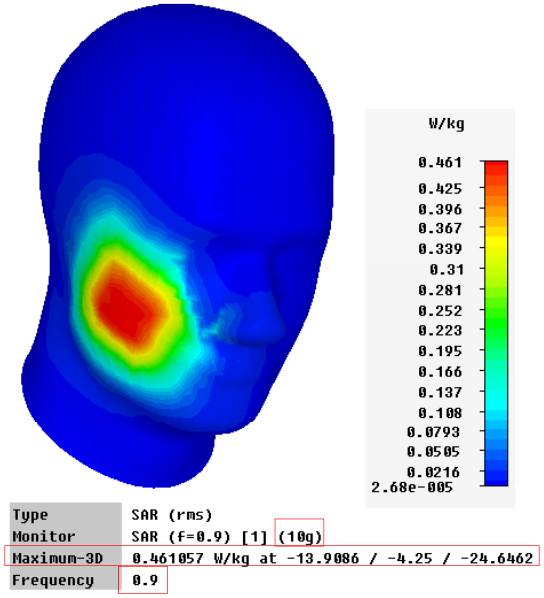

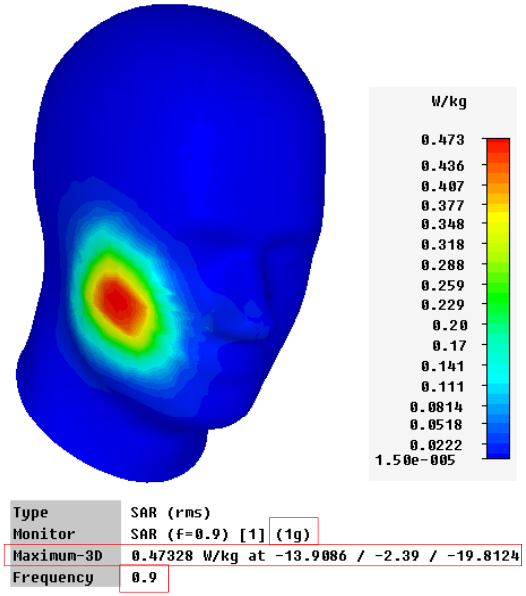

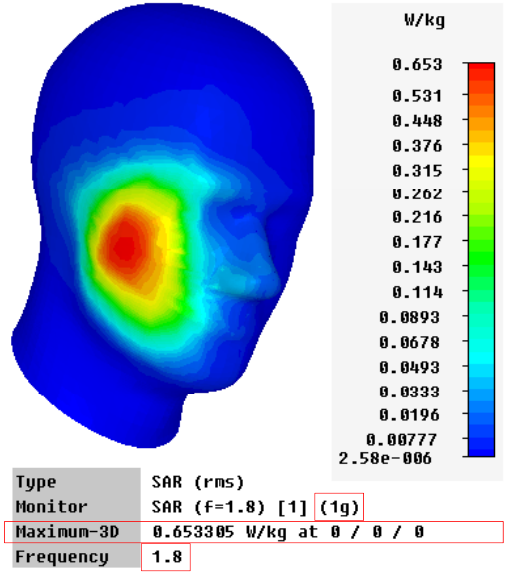

$$P_{\substack{antenna\\input}} = 1W$$

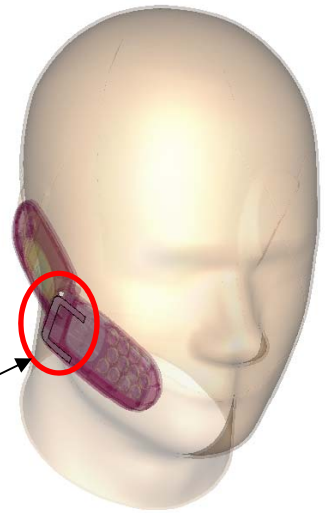

Planar Inverted F Antenna

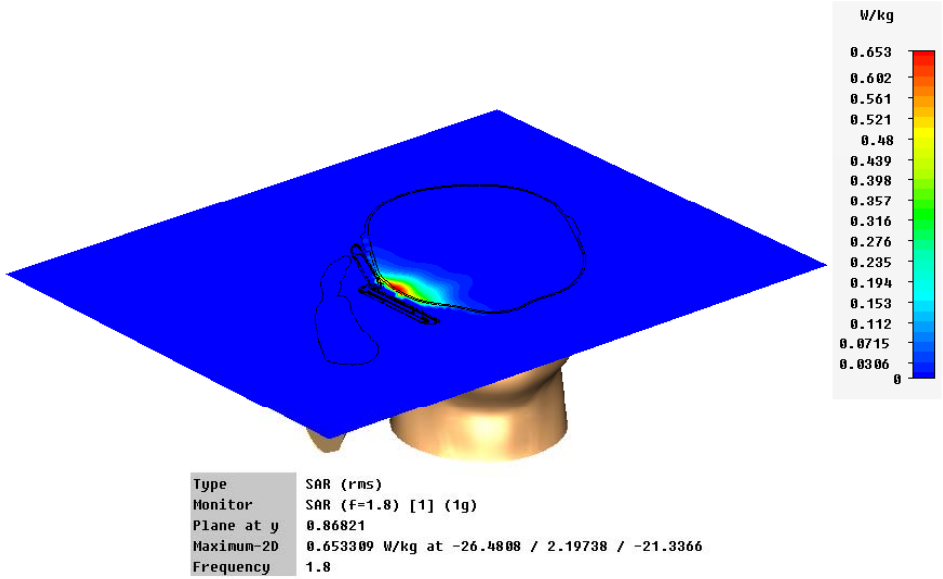

Average Specific Absorption Rate (SAR_{av})

Since biological tissues are not homogenous and their density and internal field depend on the tissue characteristics, an average SAR is also introduced:

$$SAR_{AV} = \frac{1}{V}\iiint_V \frac{\sigma(\underline{r})\left|\underline{E}(\underline{r})\right|^2}{2\rho(\underline{r})}dV \quad [W/Kg]$$

Average Specific Absorption Rate

✓ it can be measured easier than the local SAR

✓ it gives the amount of heat released to the body and then gives an idea of the thermal stress to which an organism is subjected.

✓ if V is the entire body volume, it becomes "SAR whole body".

✓ if the density can be approximated with a constant value (and $M=\rho V$):

$$SAR_{AV} = \frac{1}{\rho V}\iiint_V \frac{\sigma(\underline{r})\left|\underline{E}(\underline{r})\right|^2}{2}dV = \frac{P}{M} \qquad \left(P = \iiint_V \frac{\sigma(\underline{r})\left|\underline{E}(\underline{r})\right|^2}{2}dV \text{ [W]}\right)$$

➢ While SAR_{AV} provides the average amount of the heat released to a body (or part of it), the local SAR expresses the power dissipated in an arbitrarily small volume of tissue.

➢ Knowing local SAR distribution in a biological system allows to detect local power concentrations (hot spot) in particular areas of the body.

Normalized Specific Absorption Rate (NSAR)

NSAR is the specific absorption rate normalized to the incident power density $S^i = \left|\underline{E}^i\right|^2 / 2\zeta_0$

$$NSAR = \frac{SAR(S_0)}{S_0} \quad \left[(W/Kg)/(mW/cm^2)\right]$$

Normalized Specific Absorption Rate

For an incident power density S it comes that: $SAR = NSAR \cdot S$

SAR is linearly proportional to the incident power density (is proportional to the square of the incident field amplitude)

Specific Absorption Rate limits (examples)

SAR measures exposure to fields between 100 kHz and 10 GHz.

The SAR value is then measured at the location that has the highest absorption rate in the entire head, which in the case of a mobile phone is often as close to the phone's antenna as possible.

SAR is commonly used to measure power absorbed from mobile phones and during MRI scans. Various governments have defined safety limits for exposure to RF energy produced by mobile devices that mainly exposes the head or a limb for the RF energy:

- United States: the FCC requires that phones sold have a SAR level at or below 1.6 watts per kilogram (W/kg) taken over a volume containing a mass of 1 gram of tissue.
- European Union: CENELEC specify SAR limits within the EU, following IEC standards. For mobile phones, and other such hand-held devices, the SAR limit is 2 W/kg averaged over 10 g of tissue (IEC 62209-1).

ICNIRP guidlines:

- for general public exposure to EM fields: for whole body exposure there is a limit of 0.08 W/kg; local exposure: SAR_{AV}<2 W/Kg, average on 10g.
- SAR_{WB} limit is raised to 0.4 W/Kg for occupational/controlled exposure; local exposure: SAR_{AV}<10 W/Kg, average on 10g.

Specific Absorption Rate limits (examples)

For Magnetic Resonance Imaging the limits (in IEC 60601-2-33) are slightly more complicated:
(a) Local SAR is determined over a mass of 10 g.
(b) The limit scales dynamically with the ratio "exposed patient mass / patient mass":
NORMAL OPERATING MODE: Partial body SAR = 10 W/kg – (8 W/kg * exposed patient mass / patient mass)
(c) In cases where the orbit is in the field of a small local RF transmitt coil, care should be taken to ensure that the temperature rise is limited to 1 °C.

Averaging time	6 minutes					
	Whole body SAR	Partial body SAR	Head SAR	Local SAR		
Body Region	whole body	exposed body part	Head	Head	trunk	extremities
Operating Mode ↓	(W/kg)	(W/kg)	(W/kg)	(W/kg)	(W/kg)	(W/kg)
Normal	2	2 - 10 (b)	3.2	10 (c)	10	20
Short term SAR	The SAR limit over any 10 s period shall not exceed three times the stated values					

As a general background information, the average power density dissipated from the human body in basal metabolic conditions is of the order of 1W/Kg.

Specific Absorption (SA) for pulses

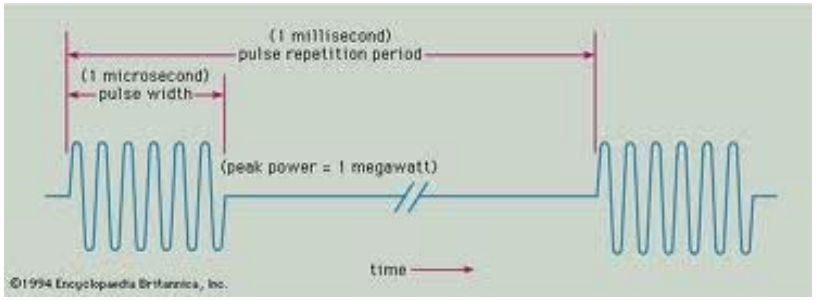

$$SA(\underline{r}) = \int_T \frac{p(t)}{\rho} dt \left[Joule / Kg \right]$$

P(t) instantaneous power density per unit volume [Watt/m^3]

SA give accounts for the energy absorbed by the body per unit mass due to the illumination by an EM pulse

Absorption Cross Section (AC)

$$P_{abs} = AC \cdot S^{inc} \qquad AC = \frac{SAR_{av} M}{S^{inc}}$$

$$\left(S^{inc} = \left| \underline{E}^{i} \right|^{2} / 2\zeta_{0} \right)$$

$$RAC = \frac{AC}{G}$$

RAC: Relative Absorption Cross Section (AC normalized with respect to the effective geometrical body section area ("silhouette")). G is around 0.43m^2 for an "average man".

Numerical dosimetry

➢ One of the most recent advances in RF/microwaves dosimetry is the availability of numerical voxel models. Realistic numerical human models are developed with medical diagnostic data, i.e., magnetic resonance imaging (MRI), computer tomography (CT).

➢ Using those voxel models a SAR distribution with millimeter resolution can be obtained.

➢ Numerical dosimetry consists in simulating the human body with a mathematical model, using mathematic relations (Maxwell's equations and proper boundary conditions) to calculate the electric and magnetic fields inside the human body.

➢ The field intensity inside the body depends on:

- the incident field parameters (frequency, amplitude, polarization)
- body shape and dimensions
- biological tissue electrical characteristics
- environmental conditions

Numerical model

➢ A theoretical model requires:

- a geometrical structure that approximates the real structure
- the physical parameters of the model (permittivity, conductivity, density)

➢ Evaluation of the internal field requires:

- incident field characterization (near or far field, frequency, polarization, intensity)
- environment characterization (presence of metallic structures, ground floor, etc.)

➢ The coupling mechanism between the EM field and the human body (or part of it) depends on the incident field wavelength and body size:

- when the maximum object dimension, L, is much less than incident field wavelength **($L<<\lambda$)**, the coupling problem can be considered as quasi-static and solved analytically: the internal field is considered to be generated by external quasi-static electric and magnetic fields (that can be considered separately).
- when the maximum object dimension, L, is much greater than incident field wavelength **($L>>\lambda$)**, the coupling problem can be solved by resorting to geometrical-optics based techniques: the electromagnetic waves are approximated by rays and the absorbed power is calculated using the wave transmission and reflection coefficients.
- when $L\sim\lambda$, a pure numerical solution is needed (differential-integral equations are solved numerically).

Analytical solution

Limitations:

- Analytical solutions of Maxwell's equations are limited to simple geometrical models (sphere, cylinder, spheroid, ellipsoid). These geometries are unable to represent a detailed human body, so relevant analytical solutions are meaningful for average-SAR estimation only.

- It is complicated to solve an EM problem where a non homogenous body is illuminated by an incident field which is different of a plane wave (this situation happens often for frequencies below a few MHz).

Advantages:

- Analytical approach furnishes explicit closed form expressions for the internal field (and SAR), as a function of frequency and polarization of the incident field, and tissue dielectric properties.

Homogenous spherical model

Consider: a homogenous sphere (which can be used to simulate the head) illuminated by a plane wave (*a* is the sphere radius which is **small with respect to the radiation wavelength**).

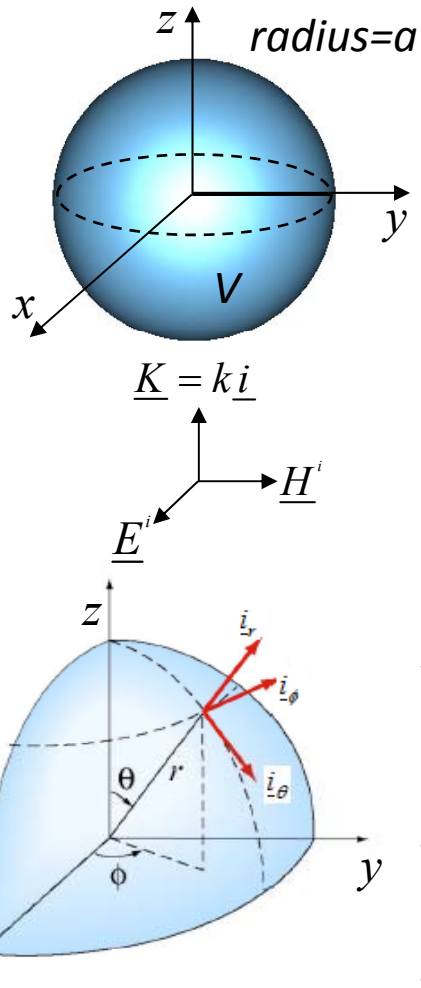

- The internal field can be expressed through a series expansion.
- If $a / \lambda_0 < 0.1$, the internal induced field can be approximated by the sum of the first two terms:

$$\underline{E} = E_0\left[\frac{3}{\tilde{\varepsilon}}\underline{i}_x + j\frac{kr}{2}\left(\cos\phi\,\underline{i}_\theta - \cos\theta\sin\phi\,\underline{i}_\phi\right)\right]$$

$$\tilde{\varepsilon} = \varepsilon' - j\varepsilon'' = \varepsilon' - j\sigma/(\omega\varepsilon_0)$$

$k=2\pi/\lambda_0$=free-space propagation constant

• the first term is the **quasi-static electric contribution**; it is uniform and has the same direction as the incident field (wave impinges from the -z-direction).

• the second term is the **quasi-static magnetic term** and is generated by the magnetic field induction (eddy currents); it is maximum at the sphere surface and decreases moving towards its center.

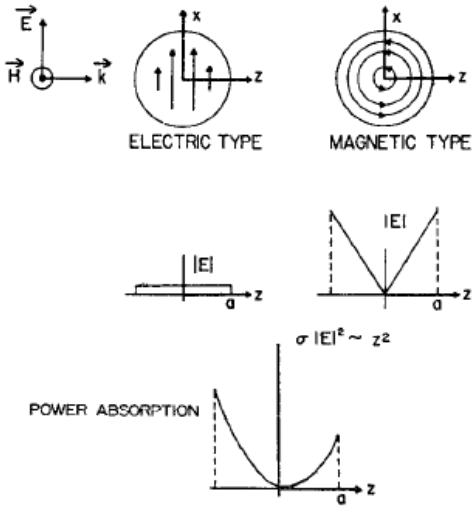

Electric field and power absorption patterns (W/m³) given by the quasi-static electric and induced magnetic solutions

J. Lin, A.W. Guy, and C.C. Johnson, "Power deposition in a spherical model of a man exposed to 1-20 MHz electromagnetic fields", *IEEE Trans. on MTT*, December 1973.

Homogenous spherical model: SAR

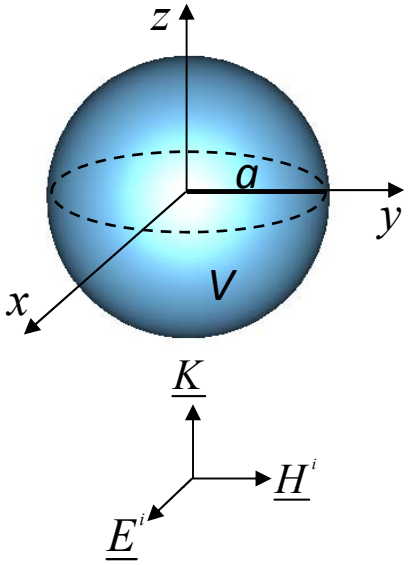

$$\underline{E} = E_0\left[\frac{3}{\tilde{\varepsilon}}\underline{i}_x - j\frac{kr}{2}\left(\cos\phi\,\underline{i}_\theta - \cos\theta\sin\phi\,\underline{i}_\phi\right)\right]$$

The **dissipated power density per unit volume** is the sum of three terms:

$$dP/dV = \frac{1}{2}\sigma\underline{E}\cdot\underline{E}^* = \frac{\sigma}{2}\left[\left|\underline{E}_E\right|^2 + \left|\underline{E}_H\right|^2 + \left(\underline{E}_E\cdot\underline{E}_H^* + \underline{E}_E^*\cdot\underline{E}_H\right)\right]$$

$\iiint_V$ =0

$$\Longrightarrow \iiint_V \quad P = \frac{\sigma}{2}E_0^2\frac{4\pi a^3}{3}\left[\frac{9}{\left|\tilde{\varepsilon}\right|^2} + \frac{2}{5}\left(\frac{ka}{2}\right)^2\right]$$

The total absorbed power is the additive sum of the quasi-static electric component and quasi-static magnetic component.

Magnetic term > electric term due to the high values of tissue permittivity, for man size models.

$$SAR_{av} = \frac{1}{\rho V}\iiint_V \frac{\sigma(\underline{r})\left|\underline{E}(\underline{r})\right|^2}{2}dV = \frac{P}{M} = \frac{\sigma}{2\rho}E_0^2\left[\frac{9}{\left|\tilde{\varepsilon}\right|^2} + \frac{2}{5}\left(\frac{ka}{2}\right)^2\right]$$

$$\varepsilon'' = \sigma/\left(\omega\varepsilon_0\right) >> \varepsilon' \quad \Longrightarrow \quad \frac{1}{k^2\left|\tilde{\varepsilon}\right|^2} = \frac{1}{\omega^2\mu_0\varepsilon_0\left(\varepsilon''\right)^2} = \frac{1}{\omega^2\mu_0\varepsilon_0\left(\sigma/\omega\varepsilon_0\right)^2\sigma\zeta_0} = \frac{1}{\left(\sigma\zeta_0\right)^2}$$

$$SAR_{av} = \frac{\sigma}{2\rho}E_0^2\left[\frac{9}{\left|\tilde{\varepsilon}\right|^2} + \frac{2}{5}\left(\frac{ka}{2}\right)^2\right] \cong \frac{\sigma}{2\rho}E_0^2k^2\left[\left(\frac{3}{\sigma\zeta_0}\right)^2 + \frac{a^2}{10}\right]$$

Homogenous spherical model: numerical results

A homogeneous sphere of muscle material is chosen (radius=25cm, equivalent to a 70kg human body)

The power density is maximum on the *xz* plane with the maximum on the sphere surface along the propagation direction of the incident field (leading surface), and it is small and almost constant along the y-axis where the magnetically induced power is low.

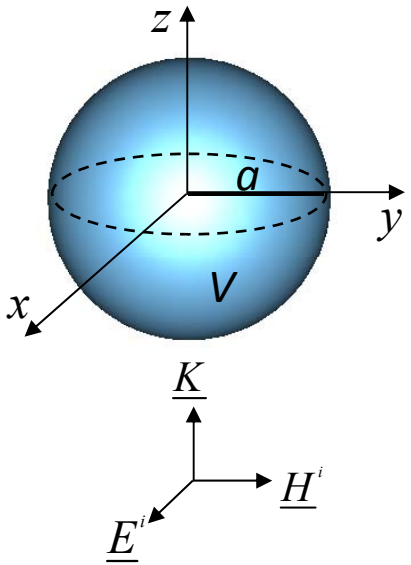

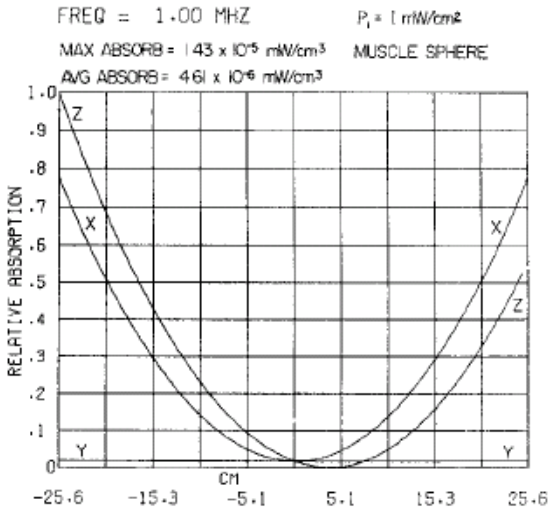

Absorbed power distributions along x, y, z axis of man-size homogenous muscle sphere in a plane wave HF field. The propagation is along the z-axis, polarization is in the x-direction

Power absorption and distribution inside a subject are functions of size. The size dependence is governed mainly from by the magnetically induced field component, since the electric coupling is independent of size. Moreover, for sufficiently small subjects the electric field contribution can be dominant (differently from what happens for a typical human size, where magnetically induced power is dominant). For a 20g mouse (radius =1.68cm) the absorption due to the magnetic and electric coupling are comparable, while for a 70 Kg man the magnetic contribution is two orders of magnitude greater than the electric one. This must be taken into account when drawing conclusions about human exposures from animal results (physical scaling).

Homogenous spherical model

- For a wave impedance $\zeta = \frac{E_x}{H_y} \neq 377\Omega$ (in antenna near-field region):

$$P = \frac{\sigma}{2} E_0^2 \frac{4\pi a^3}{3} \left[\frac{9}{|\tilde{\varepsilon}|^2} + \frac{2}{5} \left(\frac{ka}{2\zeta_{norm}} \right)^2 \right] \qquad \zeta_{norm} = \frac{E_x / H_y}{377}$$

- For $\zeta_{norm} \leq 10 \left(\zeta \leq 1200\pi\Omega \right)$ the main absorption contribution is due to the magnetic field (near field characteristics are strongly related to the antenna geometry). Therefore, magnetic fields must be measured to obtain any estimate of the hazards due to HF exposure.
- The magnetically induced energy absorption increases monotonically with the square of frequency in the HF band.
- Homogenous sphere model allows to evaluate the absorbed EM power as a function of:
  - frequency and intensity of the incident field, object size, dielectric properties of the biological tissue (permittivity, conductivity)
- This simple model can be used to get a quantitative estimate of the effect of the body volume on EM power absorption (the internal distribution of the absorbed power is less useful since the spherical model cannot account for SAR distribution at limbs. hands, etc.). When used to model the human head (radius around 7cm), the approximate results for the spherical model can be used up to 100MHz.
- Homogenous sphere model is not appropriate to represent the human body, since it doesn't take into account that the SAR is dependent on the incident field polarization (due to its spherical symmetry).

Prolate spheroidal model: polarization effects

➢ Prolate spheroid is a more appropriate model for the human body (It is obtained by rotating an ellipse around one of its principal axes).

➢ Three polarization cases are possible (the semi- length of the major axis is denoted by *a, a>b*).

Approximate solutions can be obtained at low frequencies (a/λ_0<0.1) by using a perturbation technique (series expansion with respect to free-space propagation constant $k=2\pi/\lambda_0$)

E polarization ($E^i \parallel a$)

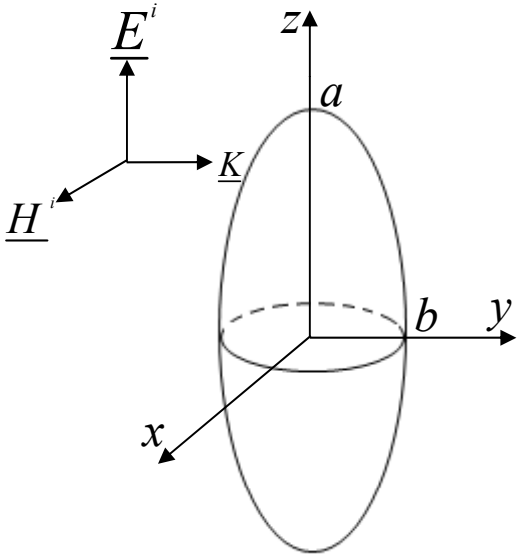

K polarization ($K^i \parallel a$)

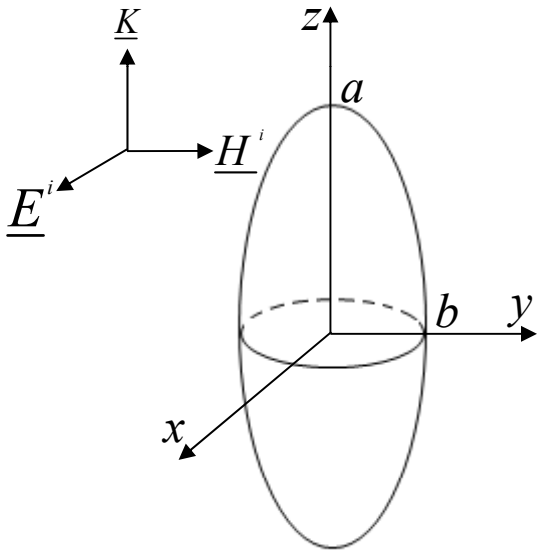

H polarization ($H^i \parallel a$)

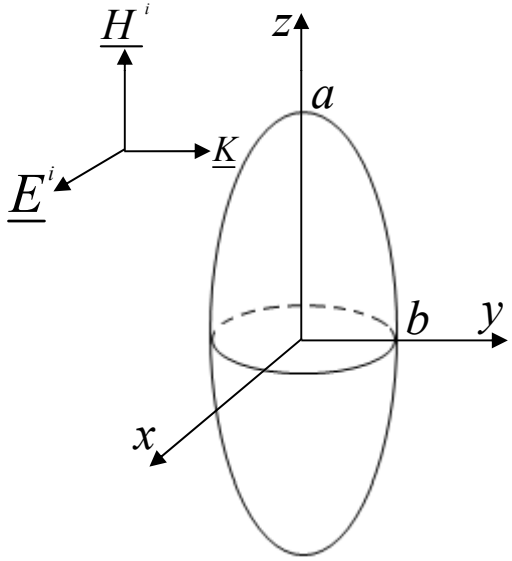

C.C. Johnson, C.H. Durney, H. Massoudi, "**Long-wavelength** electromagnetic power absorption in prolate spheroidal models of man and animals", *IEEE Trans. On MTT*, vol. MTT-23, no.9, pp. 739-747, September 1975.

Prolate spheroidal model: qualitative considerations

$$V_{spheroid} = \frac{4\pi ab^2}{3}$$

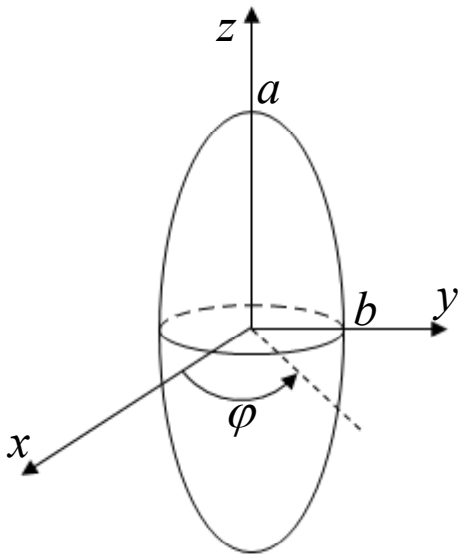

The internal field depends on the boundary conditions at the body surface.

- For H and K polarizations, boundary conditions for normal electric component mainly control the coupling mechanism:

$$\tilde{\varepsilon}\underline{E}\cdot\underline{i}_n = \left(\underline{E}^i + \underline{E}^{scattered}\right)\cdot\underline{i}_n, \left|\tilde{\varepsilon}\right| > 1$$

low electric coupling (internal field is lower than external field)

- For E polarization, boundary conditions for tangential components are more important:

$$\underline{E}\cdot\underline{i}_t = \left(\underline{E}^i + \underline{E}^{scattered}\right)\cdot\underline{i}_t$$

high electric coupling

Also consider that power absorption related to magnetic induction currents is larger when the magnetic induction is normal to larger body sections as those containing the z plane (high magnetic coupling)

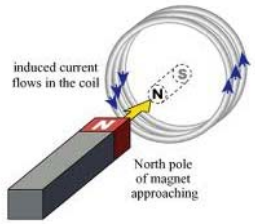

- ✓ maximum absorbed power for E polarization (E and H coupling are both high)
- ✓ minimum absorbed power for H polarization (E and H coupling are both low)

A principal conclusion from the prolate spheroid results is that the orientation of the body with respect to the incident plane wave vectors is an extremely important variable which can make an order-of-magnitude difference in EM power absorption.

Prolate spheroidal model: SAR

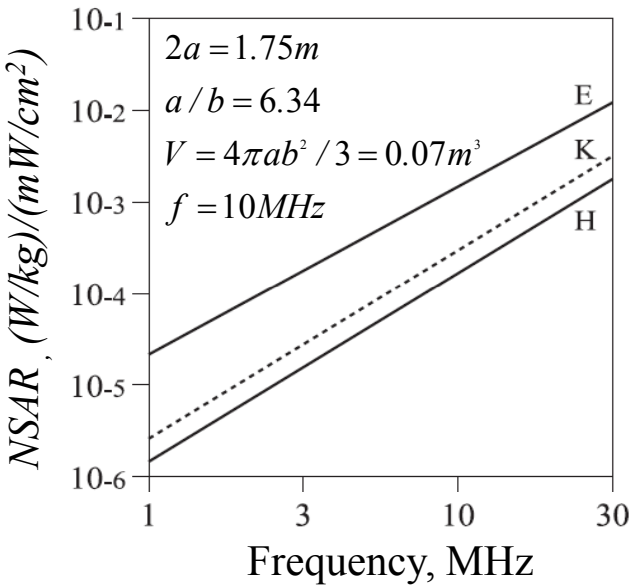

(equivalent to a 70kg human body, assumed tissue density=1g/cm^3)

$$SAR_{av}^{E} = \frac{\sigma}{2\rho} E_0^2 k^2 \left[\left(\frac{Q_E}{\sigma \zeta_0} \right)^2 + \frac{a^2 b^2}{5\left(a^2 + b^2\right)} \right]$$

$$SAR_{av}^{H} = \frac{\sigma}{2\rho} E_0^2 k^2 \left[\left(\frac{Q_H}{\sigma \zeta_0} \right)^2 + \frac{b^2}{10} \right]$$

$$SAR_{av}^{K} = \frac{\sigma}{2\rho} E_0^2 k^2 \left[\left(\frac{Q_K}{\sigma \zeta_0} \right)^2 + \frac{a^2 b^2}{5\left(a^2 + b^2\right)} \right]$$

Q_E, Q_H, Q_K - depend on the model geometry

$$k = 2\pi / \lambda_0$$

(previous equations reduce to SAR value for the spherical model when b=a)

SAR_{av} increases linearly with the square power of the frequency

SAR_{av} - maximum for E polarization
- minimum for H polarization (one order of magnitude less)

Relative absorbed power density along the x,y and z axes of a prolate spheroid

The maximum absorbed power density is <u>6.14x10-3W/kg</u> for a 1mW/cm2 incident power density

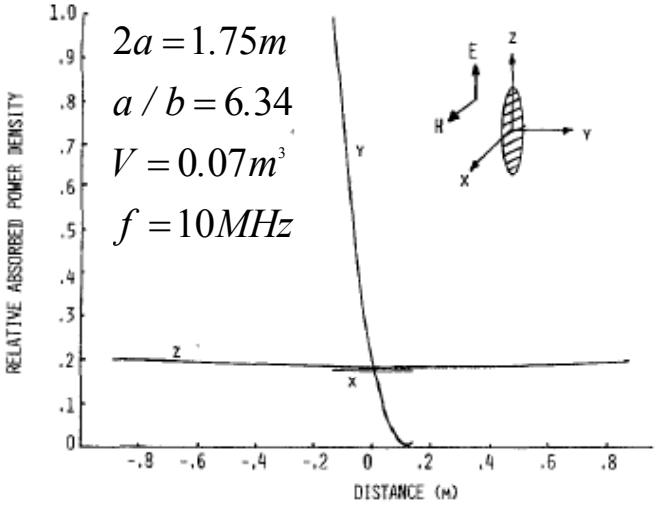

E - polarization.

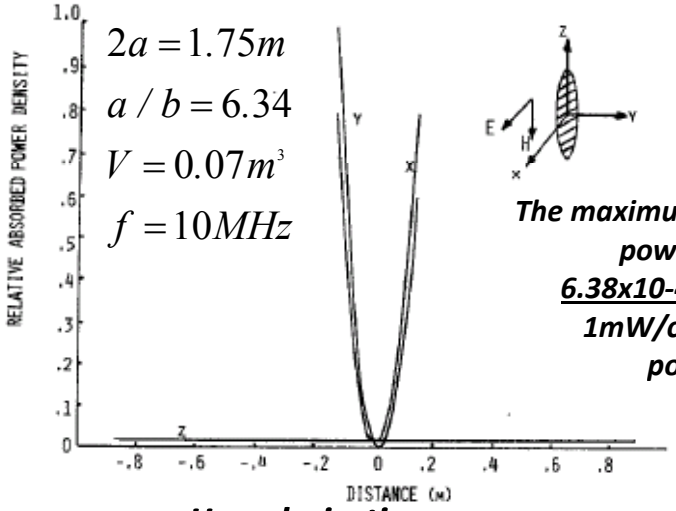

The maximum absorbed power density is <u>6.38x10-4W/kg</u> for a 1mW/cm2 incident power density

H - polarization.

Homogenous prolate spheroidal model

- It provides good results up to 30MHz for the man-size spheroid.

- Prolate spheroid model provides analytical results in agreement with measured SAR results when small animals with an almost circular symmetry with respect to their body main axis were considered (rats, mice).

- A knowledge of incident power density variations corresponding to constant tissue power absorption density (SAR_{AV}) as a function of frequency is valuable to derive EM radiation safety standards.

- When the prolate spheroid model was used to model the human body, a difference between theoretical and measured results was noticed. The theoretical absorbed power is constant even if the model is rotated by 90°! Experimentally, it was observed that this rotation causes an important SAR variations in primates (monkeys), due to different "capture area" for the electric and magnetic fields.

- Then homogenous ellipsoidal model is a more appropriate model for the human body.

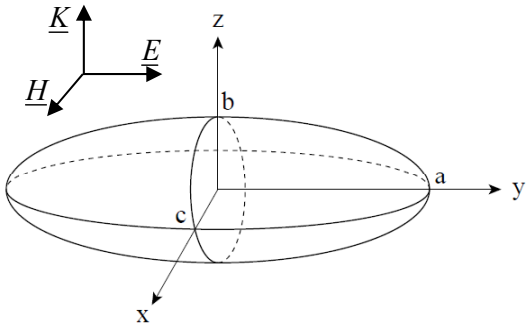

Physical scaling: example

The information given in $NSAR$ curves may be useful to extrapolate tissue-absorbed power in animal experiments to tissue absorbed power in man, under similar irradiation conditions.
For example, suppose that a biological effect is discovered in a mouse at an incident power density S=10W/cm^2 with E-polarization at 20 MHz. From Figure A, the SAR_{AV} in this case is around 2.5 W/Kg.

If the biological effects were related to average absorbed power density, it is expected to see a similar effect in man at about the same average absorbed power density (SAR_{AV} =2.5 W/Kg).

Without the information given by the analytical results in Figures A and B, one might at first conclude that the same effect would be seen in man irradiated with the same incident power density (S=10W/cm^2).

However, from Figure B it can be seen that at 20 MHz the SAR_{AV} in man irradiated by S=10W/cm^2 with E-pol is around 67W/Kg (27 times greater than that of the mouse!). Then the same SAR_{AV}=2.5 W/kg as that in the moue at S=10W/cm^2 is expected in a man at an incident power density S=10 /27=370mW/cm^2.

Average and peak absorbed power density in a prolate spheroid model of a mouse, for the three polarizations. a/b=2, a=0.0268m, V=0.00002m^3. S^i=1mW/cm^2.

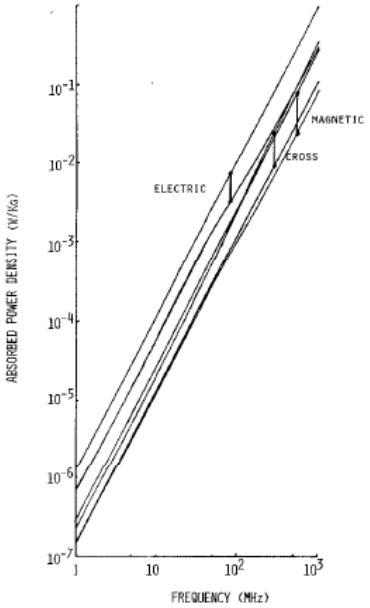

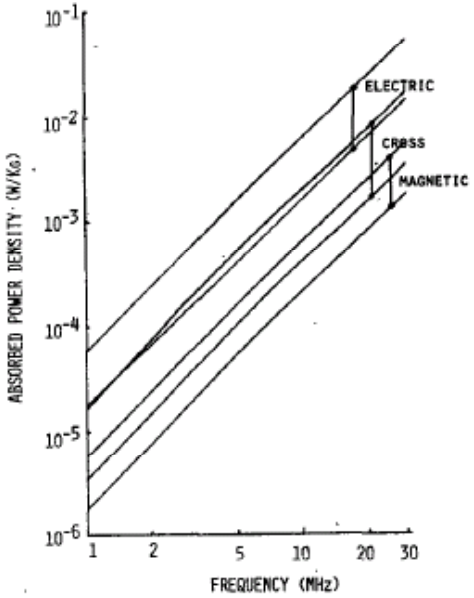

Average and peak absorbed power density in a prolate spheroid model of man, for the three polarizations. a/b=6.34, a=0.875m, V=0.07m^3. S^i=1mW/cm^2.

Homogenous ellipsoidal model $a > b > c$

Six different polarization cases are possible (ex: EKH polarization means that E, propagation direction and H are parallel to the major axis, intermediate axis, and minor axis, respectively).

EKH polarization ($E^i \parallel a \;\&\; H^i \parallel c$)

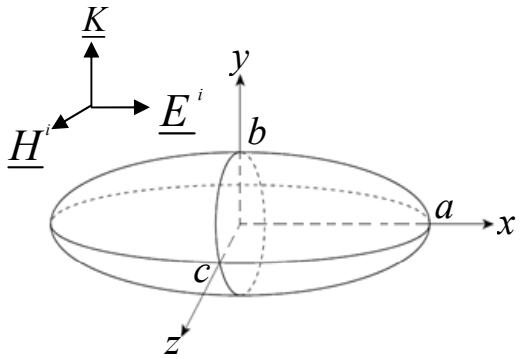

EHK polarization ($E^i \parallel a \;\&\; H^i \parallel b$)

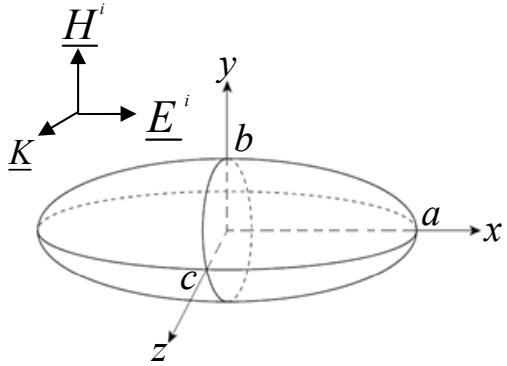

KEH polarization ($E^i \parallel b \;\&\; H^i \parallel c$)

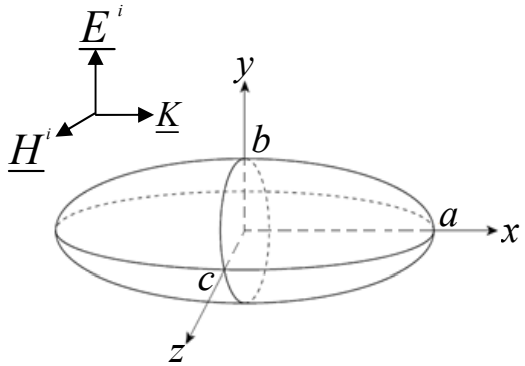

KHE polarization ($E^i \parallel c \;\&\; H^i \parallel b$)

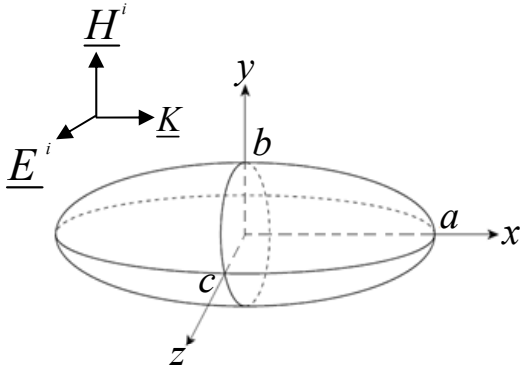

HEK polarization ($E^i \parallel b \;\&\; H^i \parallel a$)

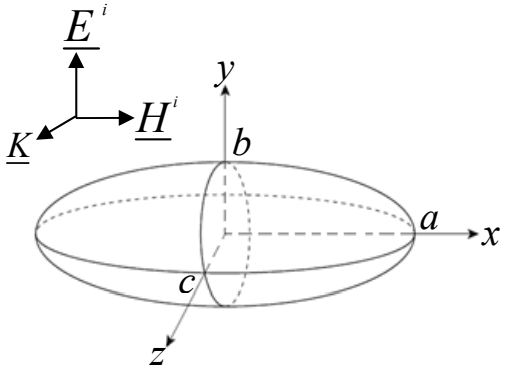

HKE polarization ($E^i \parallel c \;\&\; H^i \parallel a$)

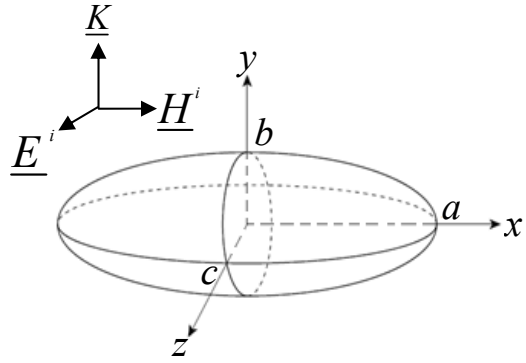

H. Massoudi, C.H. Durney, C.C. Johnson, "Long-wavelength electromagnetic power absorption in ellipsoidal models of man and animals ", *IEEE Trans. On MTT*, vol. MTT-25, no.1, pp. 47-52, January 1977.

Homogenous ellipsoidal model

$$SAR_{av}^{x} = \frac{\sigma}{2\rho} E_0^2 k^2 \left[\left(\frac{f_x(a,b,c)}{\sigma \zeta_0} \right)^2 + g_x(a,b,c) \right]$$

$$\tilde{\varepsilon} = \varepsilon' - j\varepsilon'' = \varepsilon' - j\sigma / (\omega \varepsilon_0)$$

$$k = 2\pi / \lambda_0$$

x denotes one of the six polarization cases

E_0 – magnitude of the incident field

$f_x(a,b,c)$ and $g_x(a,b,c)$ – depend on the model geometry (are different for each polarization case)

SAR_{av} increases linearly with the square power of the frequency

$2a = 1.75m$

$b/c = 2$

$V = 4\pi abc/3 = 0.07m^3$

$\sigma = 0.6S/m$

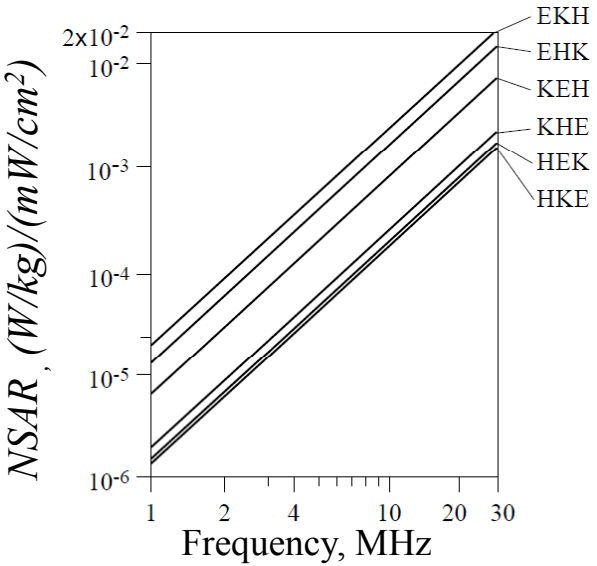

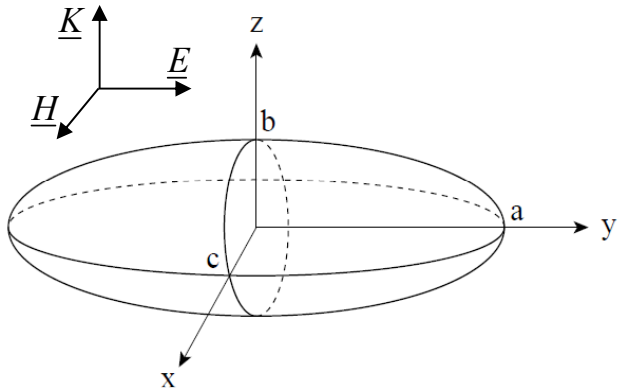

Maximum electric coupling for $E \perp a$

and maximum magnetic coupling for $H \perp c$

maximum absorption for *EKH* polarization
(minimum absorption for HKE polarization)

Polarization *EKH*

➢ For polarization *EKH* (maximum coupling):

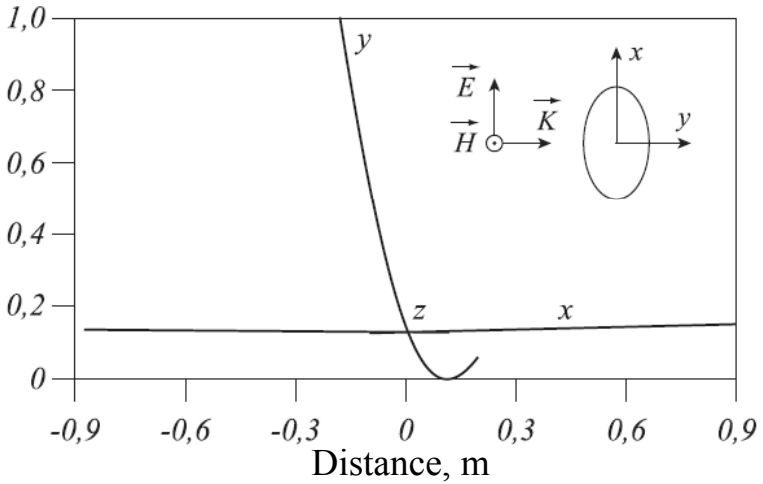

Relative absorbed power density along x, y, z – EKH polarization

-the specific absorption power is caused by an electrically induced field along x-axis combined with a magnetically induced field circulating around the z-axis (which are the eddy currents)

- since the eddy currents are zero on the z-axis, the specific absorption power is mainly due to the electrically induced field
- along x and y axis, the absorbed power is caused by a combination between electrically and magnetically induced fields.
- along x- the absorbed power is relatively flat indicating a strong electrically induced field, with relatively weak magnetically induced field because of the smaller intercepted magnetic flux.
- along y – indicates a dominant magnetically induced field, with peak power absorption on the surface of the ellipsoid (leading surface).

➢ For 20 monkeys and f=40MHz:

Ellipsoid model: a=0.14m; b=0.094m; c=0.063m; σ=0.092S/m		
Polarization	Total absorbed power	
	Measured	Calculated
EKH	847	845
EHK	832	819
KEH	376	328
HEK	360	300
KHE	166	138
HKE	162	134

Homogenous infinite cylinder

➢ Analysis on spheroidal and ellipsoidal models showed that the internal field, distribution patterns of absorbed energy, and SAR_{WB} are strong functions of the spheroid and ellipsoid orientation with respect to the vectors of the incident plane wave (and body size too). Moreover, they provide good results up to 30MHz.

➢ An numerical technique applied to a spheroid model predicted a resonance frequency near 70MHz (for a "standard man model" 1.75m and 70kg).

➢ At frequencies below the geometric-optics techniques (below 20GHz), the SAR data for the infinite cylinder calculated by an exact solution give useful results.

Consider: • an infinitely long, lossy cylinder irradiated by an EM plane wave, travelling perpendicularly to the cylinder axis

• two polarization cases are possible: E polarization ($E^i \parallel cylinder\ axis$) and H polarization ($H^i \parallel cylinder\ axis$)

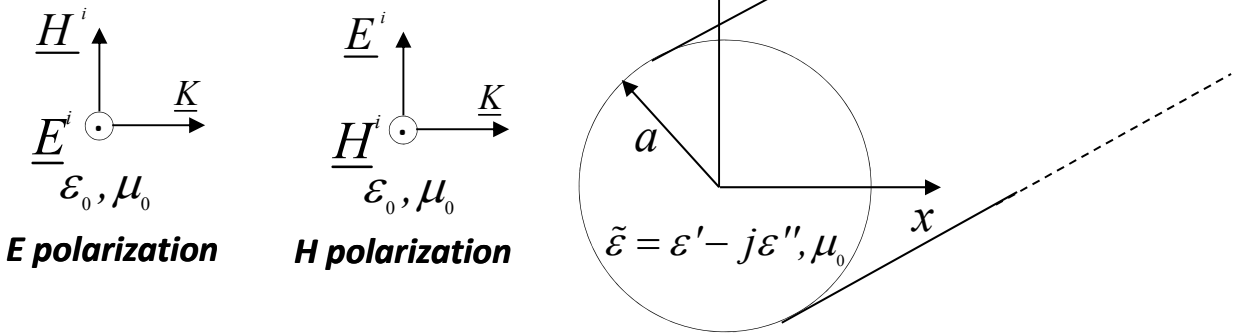

E polarization ***H polarization***

H. Massoudi et al, Radio Science, vol.14, no. 6S, pp. 35-42, November-December 1979

Homogenous infinite cylinder: SAR calculation

- Two different methods are considered: an exact solution and geometrical optics.

Analytical solution

$$SAR_X = \frac{\sigma}{\rho}\left|E_0\right|^2 A_X(ka)$$

- X – E polarization or H polarization
- a – cylinder radius
- A_X – depends on the system geometry and frequency; It contains Bessel functions

Homogenous infinite cylinder: SAR calculation

- Geometrical optics

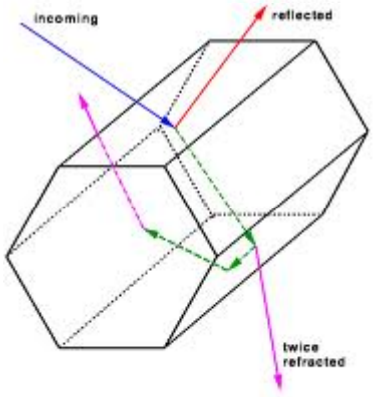

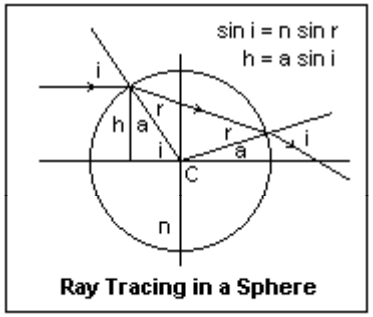

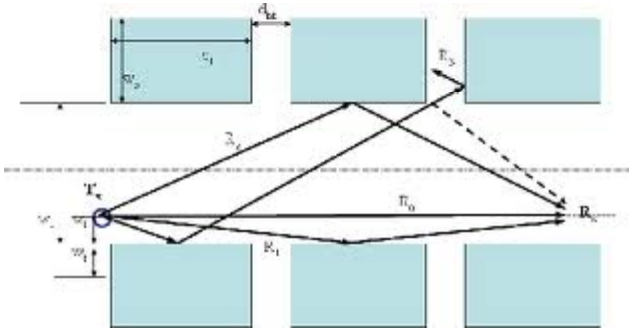

Homogenous infinite cylinder: *SAR* calculation

Geometrical-optics solution

➢ is applied when the value of the cylinder radius is much larger than that of the free-space wavelength

➢ the cylinder surface is divided into a number of thin planar subareas. The cylinder circular cross-section is firstly considered a rectangular polygon of N sides, each of length b, inscribed in a circle of radius a.

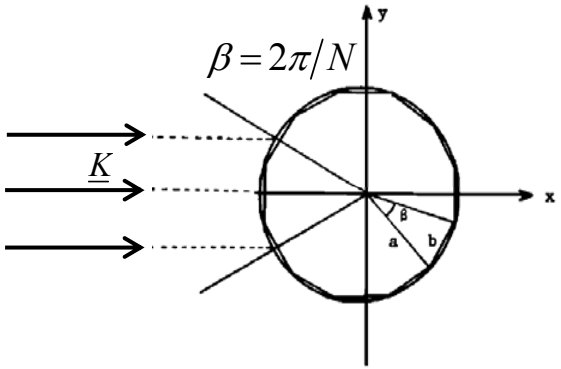

• if a uniform plane wave is incident perpendicular to the cylinder axis, each side of the polygon will see a different angle of incidence.

• the whole body rate of energy absorption is the sum of each energy transmitted in each side of the polygon.

• to calculate the rate at which energy is transmitted into each subarea, a plane wave is considered to be incident at an angle θ with the normal to the plane boundary on a dielectric interface.

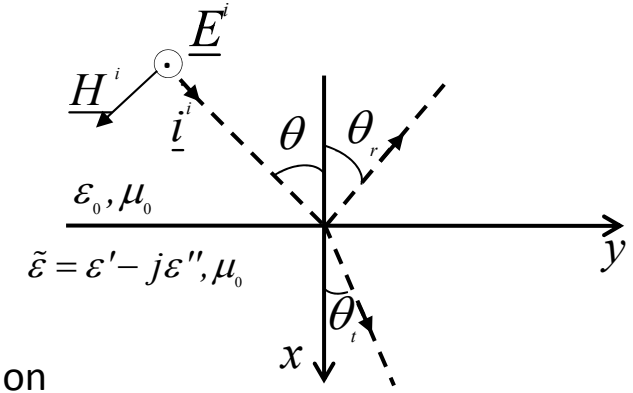

$$SAR_X = \frac{\sigma |E_0|^2}{\rho k a} A_X$$

- X – E polarization or H polarization
- a – cylinder radius
- A_X – depends on the system geometry and frequency (through permittivity values)

➢ Since the skin depth of biological tissues at high frequencies is very small, it is reasonable to assume that energy transmitted into the cylinder is completely absorbed.

Average SAR - E polarization

- SAR for cylinder model: 10MHz-5GHz- exact solution & 20GHz-100GHz- geometric-optics solution. At 10GHz both methods give similar results
- SAR for spheroidal model: low frequencies- long-wavelength analysis & higher frequencies- geometric-optics solution. The dotted lines are estimated values based on experimental values.

Average SAR in 70Kg prolate spheroidal and cylindrical models of man. Cylinder radius 11.28cm, length is 1.75m, and the spheroid has the same height as the cylinder. S^i=1mW/cm^2:

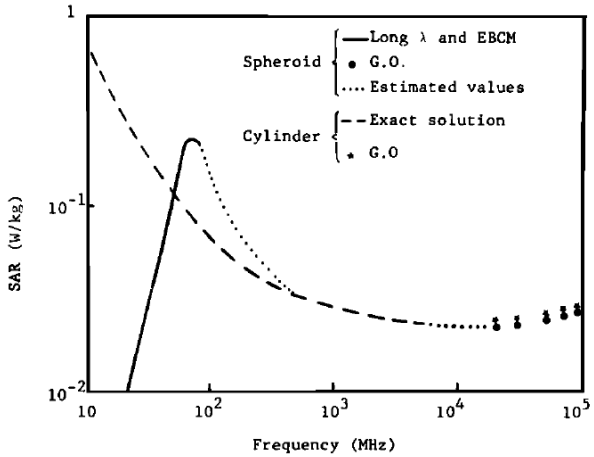

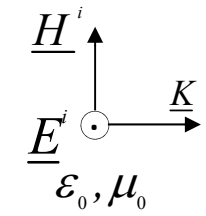

E polarization

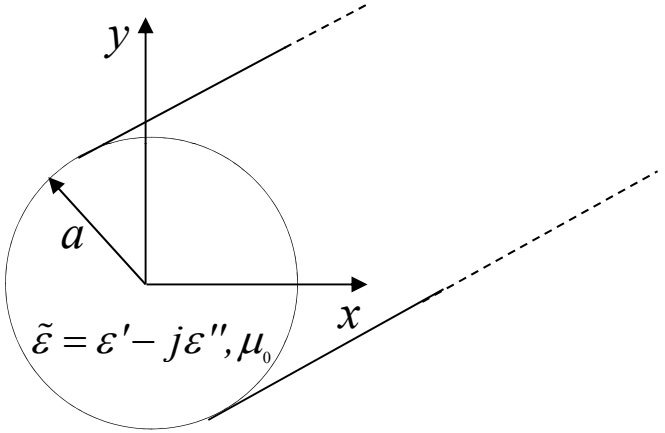

- $E^i \parallel$ *cylinder axis* and boundary conditions require that the magnitude of E be equal to that E^i of the at the boundary. Thus the coupling of the electric field in the infinite cylinder is strong. In the spheroid, the electric coupling is weaker than in the infinite cylinder due to end effects (the latter become negligible at high frequencies).
- Magnetic coupling is also stronger than in spheroid model, because in cylinder the circulating currents form closed loops at infinity (infinite cross section perpendicular to the magnetic field), while in the spheroid the circulating currents form finite closed loops.
- Since electric and magnetic coupling are higher for the infinite cylinder than spheroid, the SAR is higher in the infinite cylinder than spheroid.

Average SAR - H polarization

Average SAR in 70Kg prolate spheroidal and cylindrical models of man. Cylinder radius 11.28cm, length is 1.75m, and the spheroid has the same height as the cylinder. S^i=1mW/cm^2:

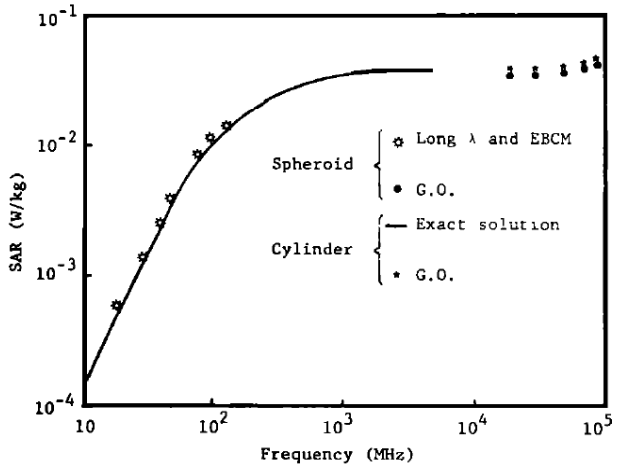

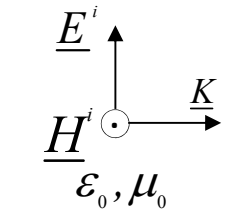

H polarization

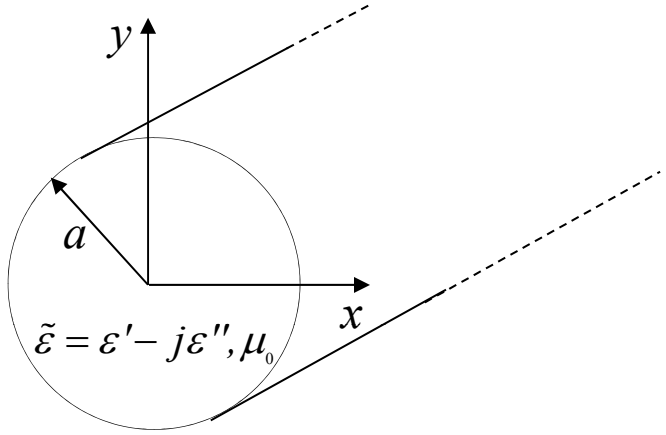

• $H^i \parallel$ *cylinder axis* and normal boundary conditions require that the magnitude of E be reduced by almost a factor of $|\varepsilon|$ (relative complex permittivity) relative to the E^i. Thus the coupling of the electric field in both models is nearly the same.

• The E field induced by the H^i forms loops which correspond to eddy currents. Since H^i lies along the long axis of both infinite cylinder and spheroid model, the induced eddy currents are nearly the same in both models, and hence the magnetic coupling is nearly the same for both models.

• For H polarization, both electric and magnetic field coupling is nearly the same in cylindrical model as it is in prolate spheroid (especially long spheroid).

• The two models have similar absorption characteristics.

Conclusions

The analytical solutions previously studied:

❑ are not suitable for radiation wavelengths between $10L$ (lower limit for quasi-static solutions, $\lambda>10L$) and $L/3$ (upper limit for cylinder model, $\lambda<L/3$): ***L/3<λ<10L*** **(c/10*L*<*f*<c3/*L*, c=3x10^{8}m/sec)**

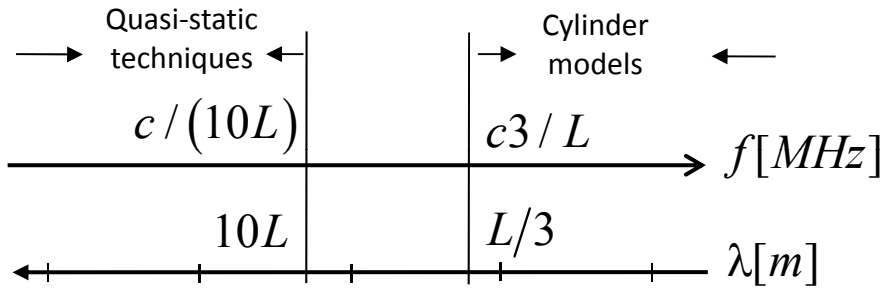

❑ they solve only homogenous problems (exception: multi-layer sphere)

❑ due to a quasi-static approximation to calculate the field equations, they fail to take into account a dimensional resonance (that appear at around $\lambda\approx 2.5L$) where an absorption peak was experimentally noticed mainly for the E polarization.

Numerical solutions

- Requires the discretization of the Maxwell's equations (integral, differential, integral-differential) in spatial domain.
- The known variables are: the incident EM field and the biological tissue characteristics.
- The unknowns are the internal fields.
- The biological body needs to be divided in discrete elements (cells).
- The size of the cells has a maximum limit depending on the wavelength (usually less than 1/10 of a wavelength)

Method of moments (MoM)
Finite Difference Time Domain (FDTD)
Finite Element Method (FEM)
Finite Integration Technique (FIT)
Etc.

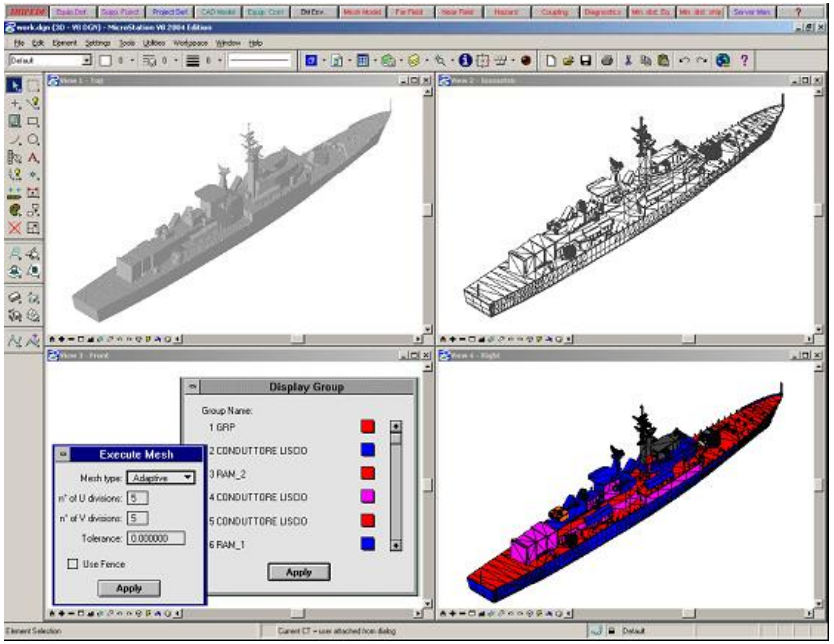

Numerical phantoms

➢A number of realistic heterogeneous human models are currently used for electromagnetic field simulations. These models are three-dimensional digital models derived from cross-sectional images of Computer Tomography (CT), Magnetic Resonance Tomography (MRI).

➢The data is represented by voxel images of thin slices of the body. The voxels usually have a resolution of 256 by 256 pixels, with each pixel corresponding to 12 bits of gray tone.

➢ Can represent the entire body or different body shapes (head, hand).

➢ Can be homogenous or inhomogeneous. Homogenous phantoms can be used for rapid numerical prototyping and are accurate enough for high frequencies. Inhomogeneous phantoms contain anatomical details of human body and are most accurate in terms of dielectric properties and geometrical information.

➢ Can represent different gender (male, female, child).

➢ May have different sizes.

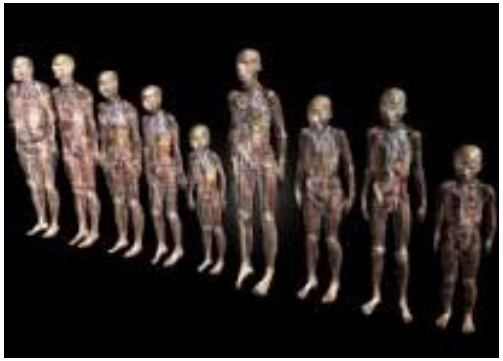

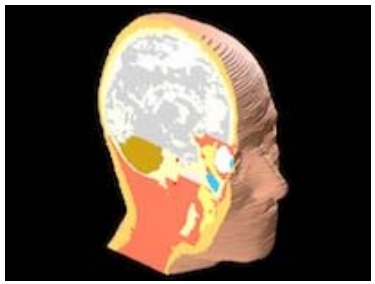

SAM phantom – homogenous phantom

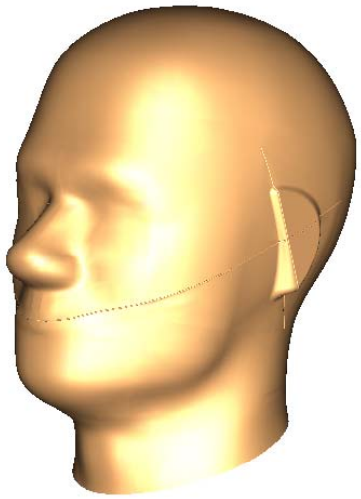

- The Specific Anthropomorphic Mannequin (SAM) corresponds to the 90th-percentile dimensions of an adult male head based on an anthropomorphic study of US Army personnel. SAM was proposed by the Subcommittee SCC34-SC2 for compliance testing of handheld devices and subsequently adopted for the drafts of IEEE 1528-200x as well as for CENELEC prEN50361.
- Tissues: homogenous material (ex: ε_r=42, σ=0.99S/m), shell (2mm).
- Resolution: 0.2mm to 1mm
- Features: Left and right ear and mouth reference points marked; standard positions predefined.

HUGO Human Body Model

- Is based on a dissected male (1.88m) corpse cuted into several thousand slices.
- The import is performed via an interface that allows different resolutions (1mm to 8mm) and different material tissues to be chosen.
- Tissues: more than 100 different tissue types distinguished.

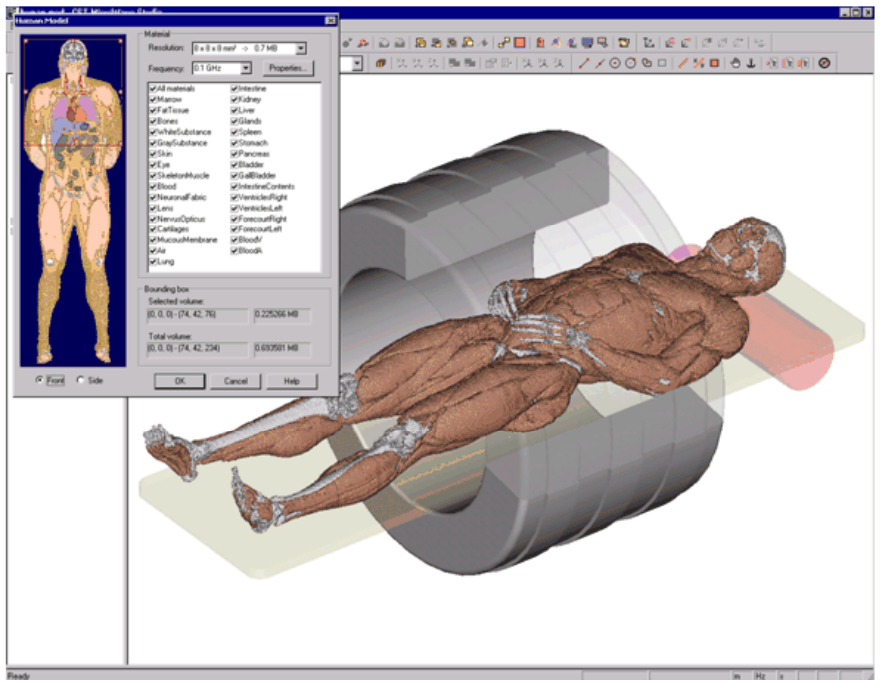

Human Body Interface - different tissues and different resolutions

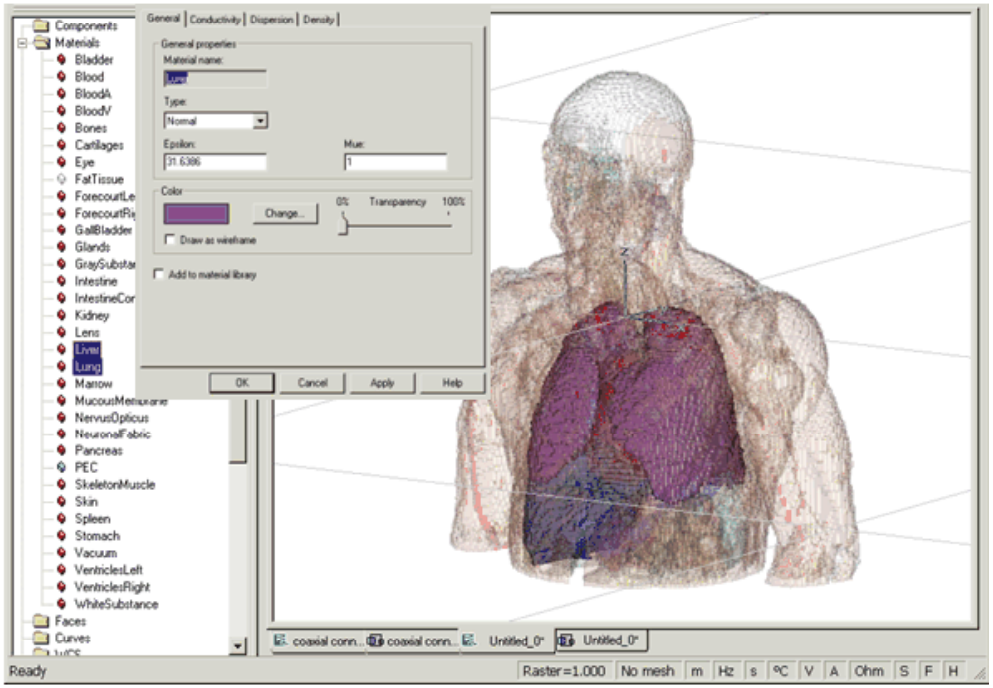

Access to the material properties

Human Head Models

European Male Head

Resolution: 0.2mm to 1.1mm
Tissues: air, skin, muscle, fat, bone, CSF, brain, blood, cartilage, vitreous humour, lens, eye sclera.

High Resolution European Female Head

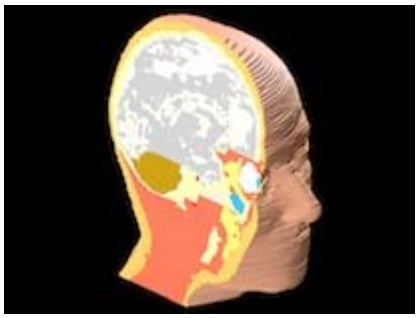

This phantom is based on a high resolution MRI scan of a healthy female volunteer (age 40) obtained from the University of Zurich. The ears were gently pressed to the head surface in order to obtain the appropriate ear shape for a realistic MTE user. 121 slices were taken. Resolution: 0.2mm to 3mm. Fifteen different tissues are distinguished.

European Child Head, Age 7

European Child Head, Age 3

Are based on real MRI data. Resolution: 0.2mm to 4mm. Fifteen different tissues are distinguished.

Japanese head model

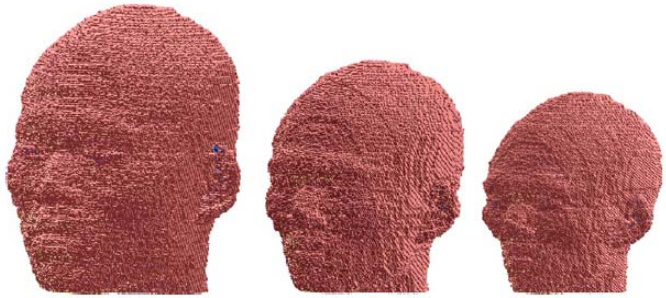

From left to right the Japanese adult head model (JPAD), the head model anatomically scaled to a 7 year old child (JP7YS), and to a 3 year old child (JP3YS). Resolution: 0.2mm to 4mm. Fifteen different tissues are distinguished.

Animal phantoms

- Rat and mouse phantoms based on MRI scans of different weight, gender (male, female, pregnant female) were developed.
- Resolution: 0.6mm to 1.1mm.
- Tissues: brain, bone, muscle, fat, skin, heart, lungs, digestive system, liver, kidneys, testicles (males) or uterus (female), eyes, nose region and others.

Method of moments (MoM) results

MoM results :

-resonances were noticed around 70MHz for vertical polarization and around 200MHz for horizontal polarization

- for the head a resonance was noticed at around 375MHz

- SAR_{av} calculated with homogenous and non homogenous models are similar

(resonances appear at around $\lambda \approx 2.5L$)

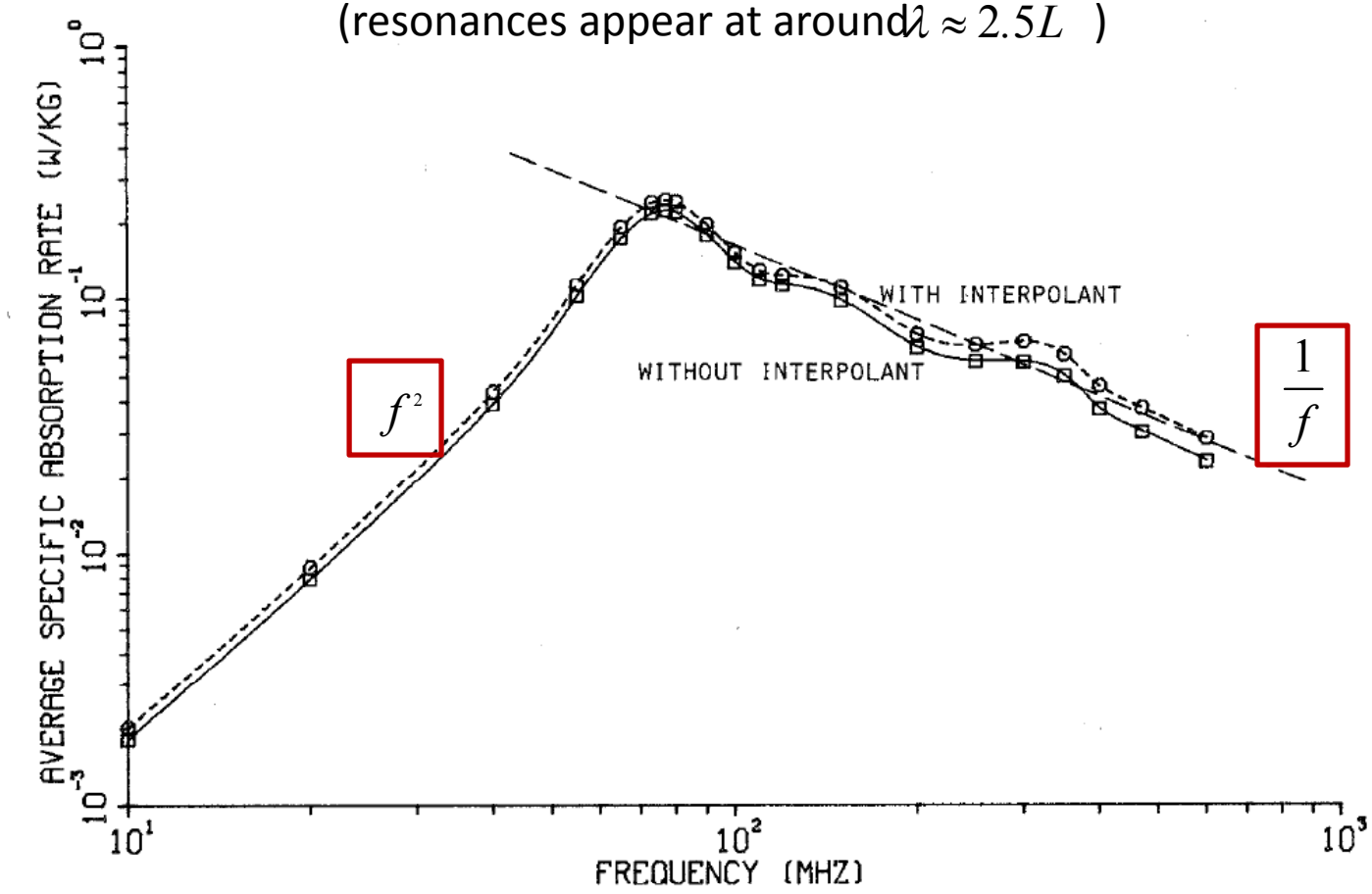

Whole Body SAR for a homogenous man model in free space, vertical electric field, incidence front-to-back, S^i=1mW/cm²

Local SAR: MoM and FDTD results

For a plane wave, vertically polarized, an incident power density of 1mW/cm^2 and a medium height man:

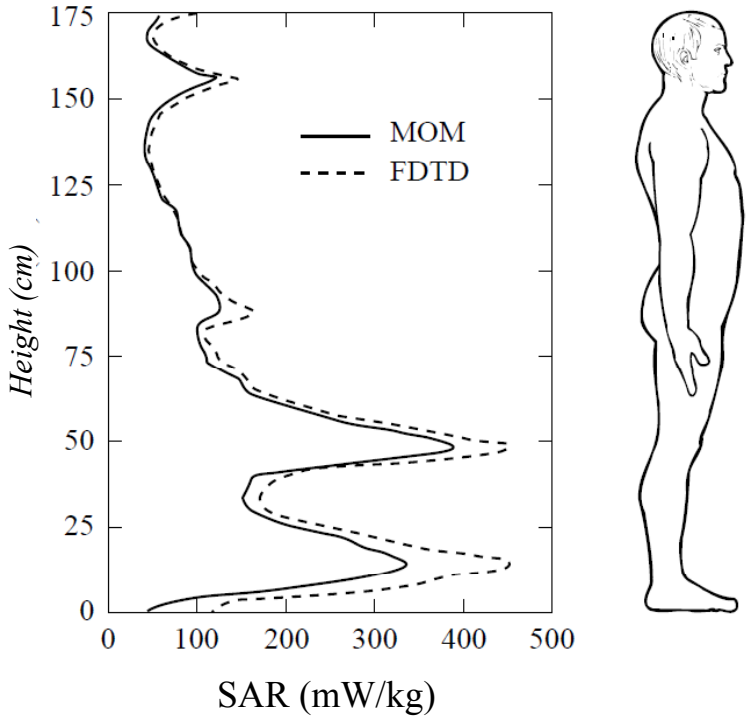

$$SAR_{WB}^{MoM} = 101 mW \ / \ kg$$

$$SAR_{WB}^{FDTD} = 116 mW \ / \ kg$$

Method of moments (MoM)

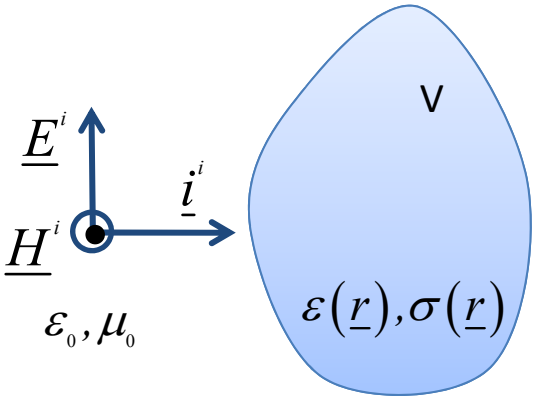

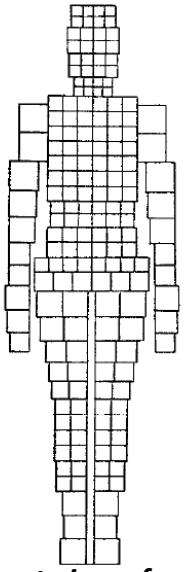

Front view of a 626-cells man model

- The internal field is related to the external field by an electric-field integral equation (EFIE).
- The EFIE can be solved with numerical methods if the radiated body is divided in small cells, where the electric characteristics and internal field are considered constants.
- If the body is divided in N block cells, the coupling problem is described with a system of N equations with N unknowns:

$$\underline{\underline{G}} \cdot \underline{\underline{E}} = \underline{\underline{E}}^i$$

- $\underline{\underline{G}}$: a matrix involving the complex properties of the body
- $\underline{\underline{E}}$: total electric field
- $\underline{\underline{E}}^i$: incident electric field

- The system solution is obtain using a numerical software and a computer.

Finite Difference Time Domain (FDTD)

- The development of mobile phones has led to focus the attention on frequencies above 900MHz (operating frequency).
- These devices produce an inhomogeneous electromagnetic field, with a strong intensity close to the antenna device. In this case, dosimetric studies were focused manly on the head and not on the whole body.
- 10% to 50% of the total power emitted by a mobile phone can be dissipated in the user's head.
- In order to better quantify the power absorbed by the head (SAR), another technique (as an alternative to MoM) can be used: "FDTD- Finite Difference Time Domain".
- The method is based on a discretization – in space and time – of the Maxwell's equations.
- The biological body is divided in many cubic cells, each of it having constant electric characteristics.

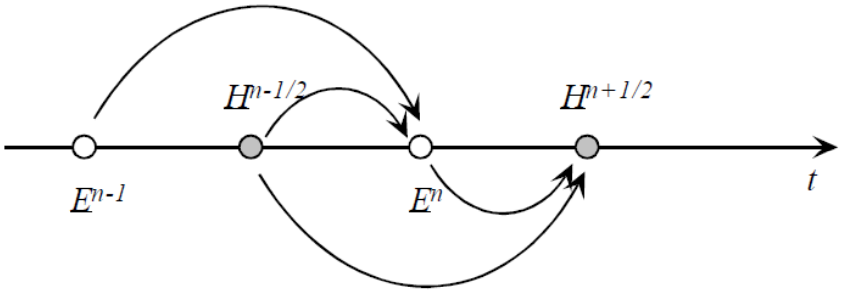

Electric field expression

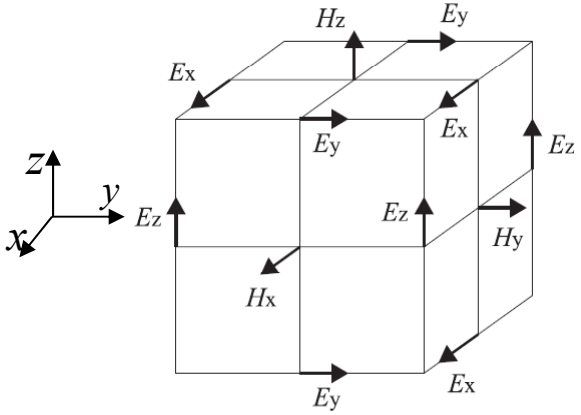

Consider the space position of a point in the human body:

$$x = i\Delta x, y = i\Delta y, z = i\Delta z$$

and the time instant:

$$t = n\Delta t$$

- The electric field at a given point at time t is obtained as a function of: electric field at the same point at a precedent time t-Δt and of magnetic field at time t-$\Delta t/2$ in four different points around the considered one.
- Similarly, the magnetic field is updated from the magnetic field produces at a previous step (t-Δt) and from the electric field produced at the intermediate step (t-$\Delta t/2$).

$$E_z^n\left(i,j,k+\frac{1}{2}\right) = f(\varepsilon,\sigma)E_z^{n-1}\left(i,j,k+\frac{1}{2}\right) + g(\varepsilon,\sigma)\Delta t\left[H_y^{n-\frac{1}{2}}\left(i+\frac{1}{2},j,k\right) - H_y^{n-\frac{1}{2}}\left(i-\frac{1}{2},j,k\right) + H_x^{n-\frac{1}{2}}\left(i,j+\frac{1}{2},k\right) - H_x^{n-\frac{1}{2}}\left(i,j-\frac{1}{2},k\right)\right]$$

depend on the body electrical characteristics

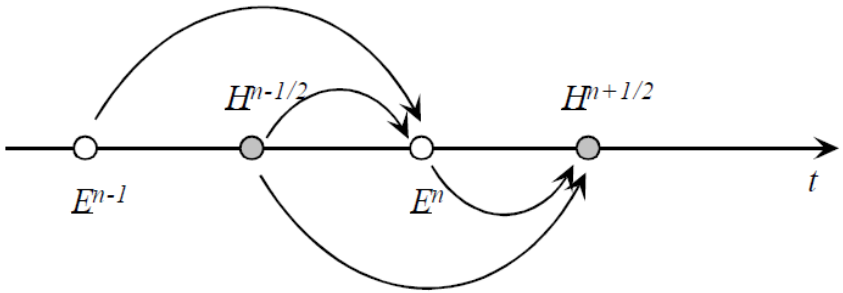

SAR of a human body

$M = 70kg$

$L = 1.75m$

$S^i = 1mW / cm^2$

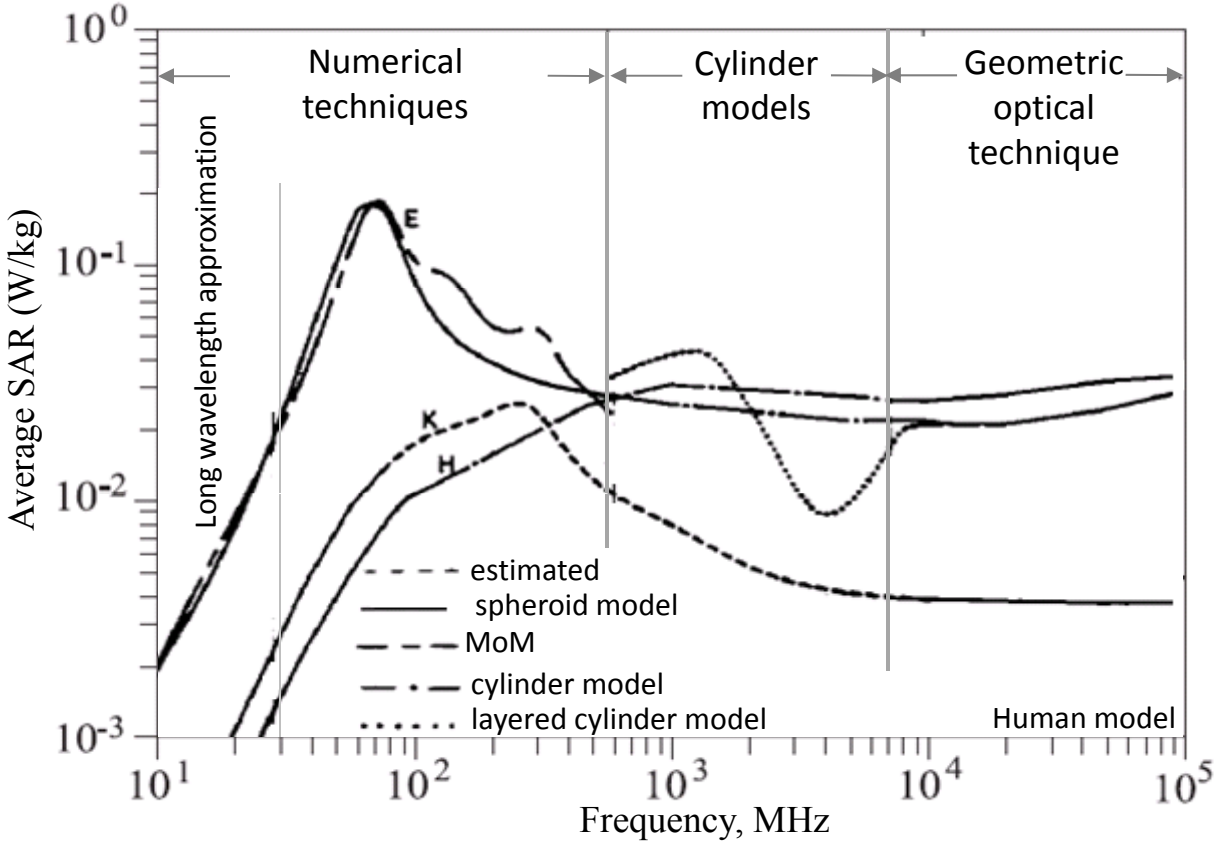

- ✓ for $L<\lambda/5$ SAR_{av} is proportional to f^2
- ✓ around resonance ($\lambda \sim 2.5L$) SAR_{av} increases more than f^2
- ✓ over the resonance SAR_{av} decreases with $1/f$.
- ✓ over the resonance maximum absorbed power occurs for E-polarization
- ✓ over the resonance minimum absorbed power occurs for H-polarization

C.H. Durney, Electromagnetic dosimetry for models of humans and animals - A review of theoretical and numerical techniques, IEEE Proceedings, vol. 68, no. 1, pp. 33-40, January 1980.

Ground effect

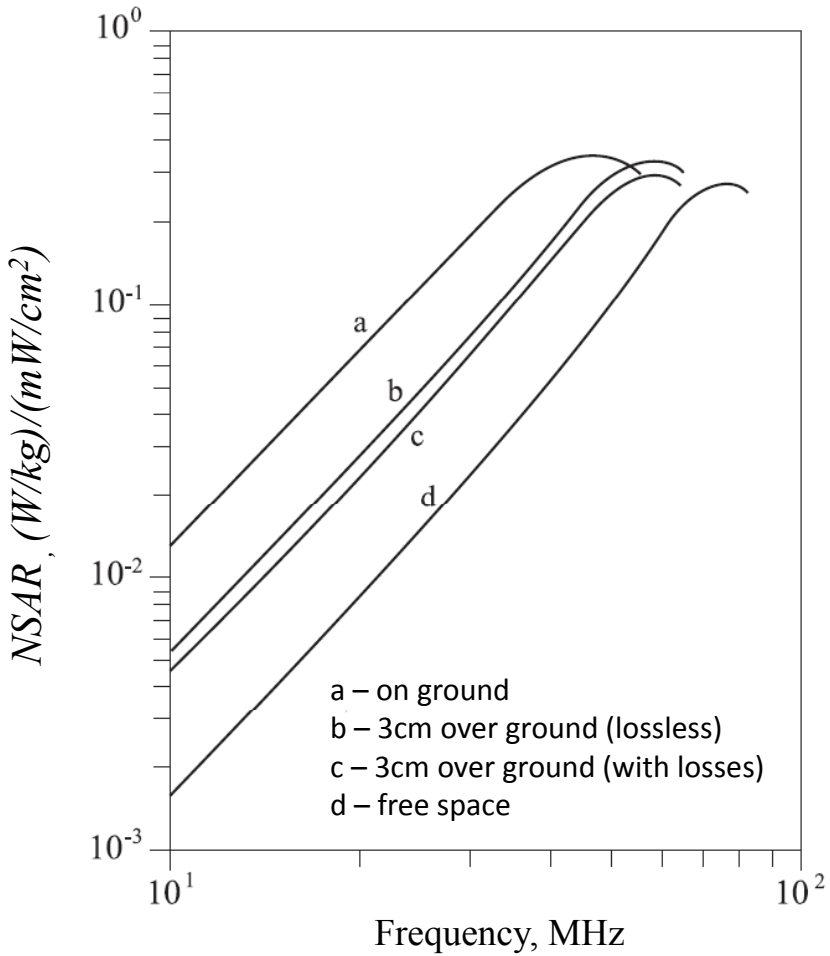

(resonances appear at around $\lambda \approx 2.5L$)

- presence of ground increases the SAR_{av} by one order magnitude
- presence of ground reduces of around 50% the value of the resonant frequency of the body in free-space

Height effect

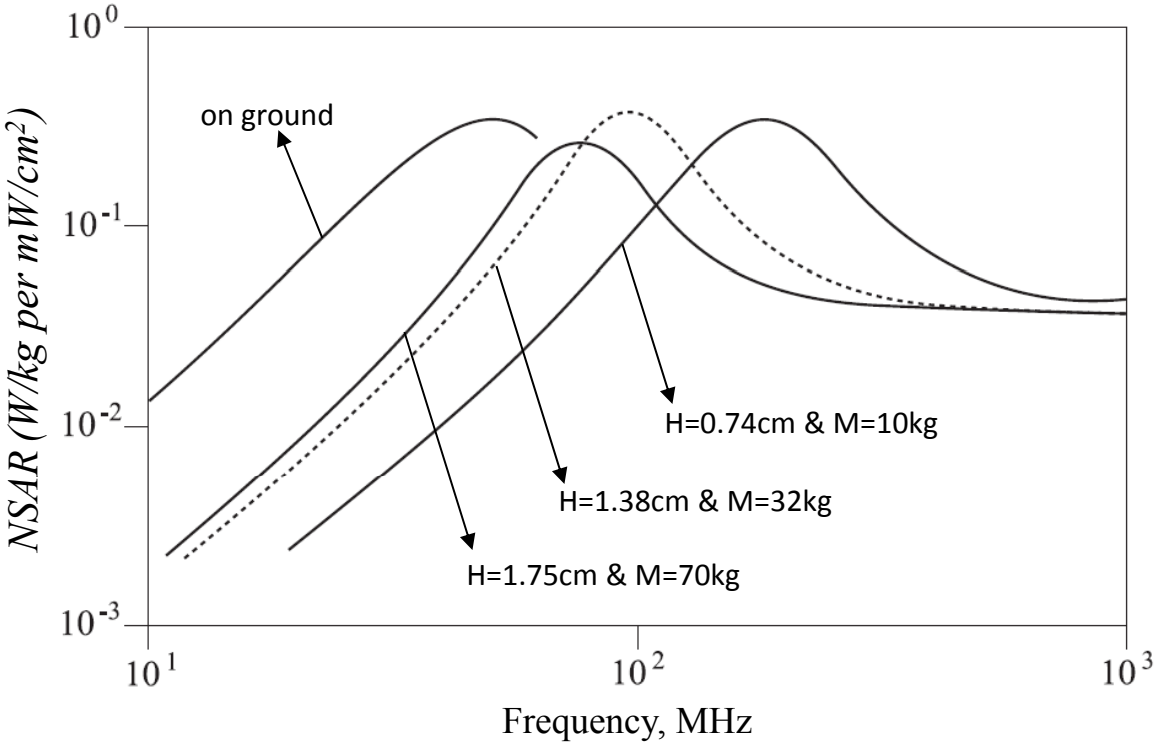

- increasing the body height the frequency resonance is shifted towards lower values
- the presence of a ground plane doubles the electrical size of the body, and as a consequence the resonance frequency is halved

(resonances appear at around $\lambda \approx 2.5L$)

Finite Integration Technique (FIT)

➢ Finite Integration Technique (FIT) provides a spatial discretization scheme, applicable to various problems, from static field calculations to high frequency applications **in time and frequency domain**.

➢ FIT method discretizes the integral form of Maxwell equations. To solve these equations a finite calculation domain enclosing the considered application problem must be defined.

➢ Uses all six vector components of electric field strength and magnetic flux density on a dual grid system. The spatial discretization of Maxwell's equations is performed on two orthogonal grid systems. Maxwell's equations are formulated for each of the cell facets separately.

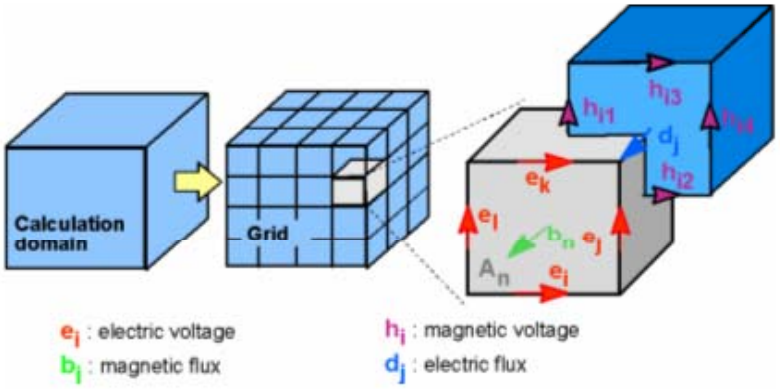

$$\oint_L \underline{e}\cdot\underline{i}_l\cdot dl = -\frac{\partial}{\partial t}\iint_S \underline{b}\cdot\underline{i}_n dS \quad \square \quad \boldsymbol{Ce} = -\frac{\partial}{\partial t}\boldsymbol{b}$$

$$e_i + e_j - e_k - e_l = -\frac{\partial}{\partial t} b_n \Rightarrow \underbrace{\begin{pmatrix} \cdots & \cdots & \cdots \\ 1 \;.\; & 1 \;.\; & -1 \;.\; -1 \\ \cdots & \cdots & \cdots \end{pmatrix}}_{\boldsymbol{C}} \underbrace{\begin{pmatrix} e_i \\ \vdots \\ e_j \\ \vdots \\ e_k \\ \vdots \\ e_l \end{pmatrix}}_{\boldsymbol{e}} = -\frac{\partial}{\partial t}\underbrace{\begin{pmatrix} \vdots \\ b_n \\ \vdots \end{pmatrix}}_{\boldsymbol{b}}$$

➢ The complete discretized set of *Maxwell's Grid Equations* (MGEs - maintain energy and charge conservation):

$$\boldsymbol{Ce} = -\frac{d}{dt}\boldsymbol{b} \qquad \tilde{\boldsymbol{C}}\boldsymbol{h} = \frac{d}{dt}\boldsymbol{d} + \boldsymbol{j} \qquad \tilde{\boldsymbol{S}}\boldsymbol{d} = \boldsymbol{q} \qquad \boldsymbol{Sb} = \boldsymbol{0}$$

Finite Integration Technique (FIT)

➢ The relations between displacement field $\boldsymbol{D}$ and $\boldsymbol{E}$, and the magnetic field $\boldsymbol{H}$ and $\boldsymbol{B}$:

$$\begin{aligned} \underline{D} &= \varepsilon \underline{E} \\ \underline{B} &= \mu \underline{H} \\ \underline{J} &= \sigma \underline{E} + \underline{J}_s \end{aligned} \quad \Longrightarrow \quad \begin{aligned} \boldsymbol{d} &= \boldsymbol{M}_{\varepsilon} \boldsymbol{e} \\ \boldsymbol{b} &= \boldsymbol{M}_{\mu} \boldsymbol{h} \\ \boldsymbol{j} &= \boldsymbol{M}_{\sigma} \boldsymbol{e} + \boldsymbol{j}_S \end{aligned}$$

➢ The time domain solver is based on the solution of the discretized set of *MGEs*:

$$\mathbf{e}^{n+1/2} = \mathrm{e}^{n-1/2} + \Delta t \mathbf{M}_{\varepsilon}^{-1} \left[\tilde{\mathbf{C}} \mathbf{M}_{\mu}^{-1} \mathbf{b}^{n} + \mathbf{j}_S^{n} \right]$$

$$\mathbf{b}^{n+1} = \mathrm{b}^{n} - \Delta t \mathbf{C} \mathbf{e}^{n+1/2}$$

➢Both types of unknowns are located alternately in time, as in the well-known leap-frog scheme:

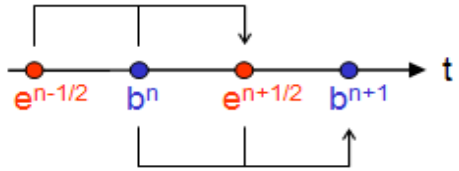

➢The magnetic flux at $t=(n+1)\Delta t$ is computed from the magnetic flux at the previous time step $t=n\Delta t$ and from the electric voltage at half a time step before, at $t=(n+1/2)\Delta t$.

SAR for Head & Hand - Mobile Phone Calculation

- This example contains a typical setup for a complete dual-band mobile phone system simulation for *SAR* calculation.
- It includes the SAM phantom head and the impact of a hand model.
- The liquid of the head phantom is defined as a broadband frequency-dependent material matching the required material properties at all frequencies of interest.
- SAR is evaluated for both frequency bands - 0.9 and 1.8 GHz.

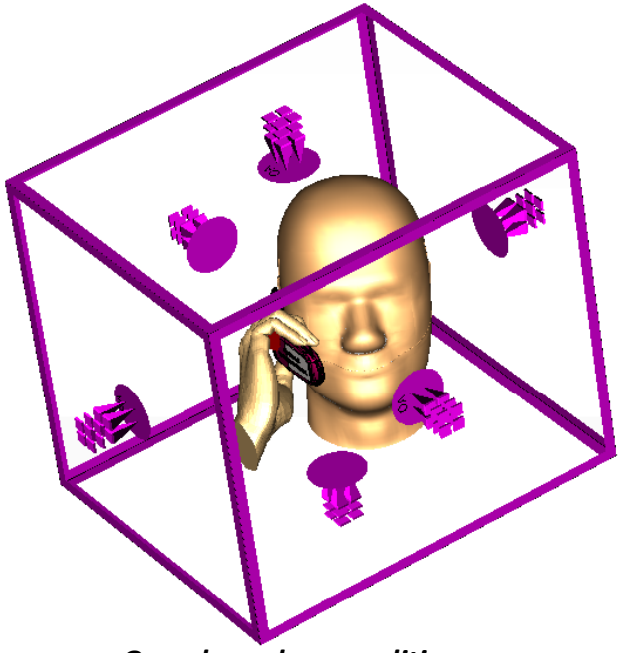

Open boundary conditions (free space)

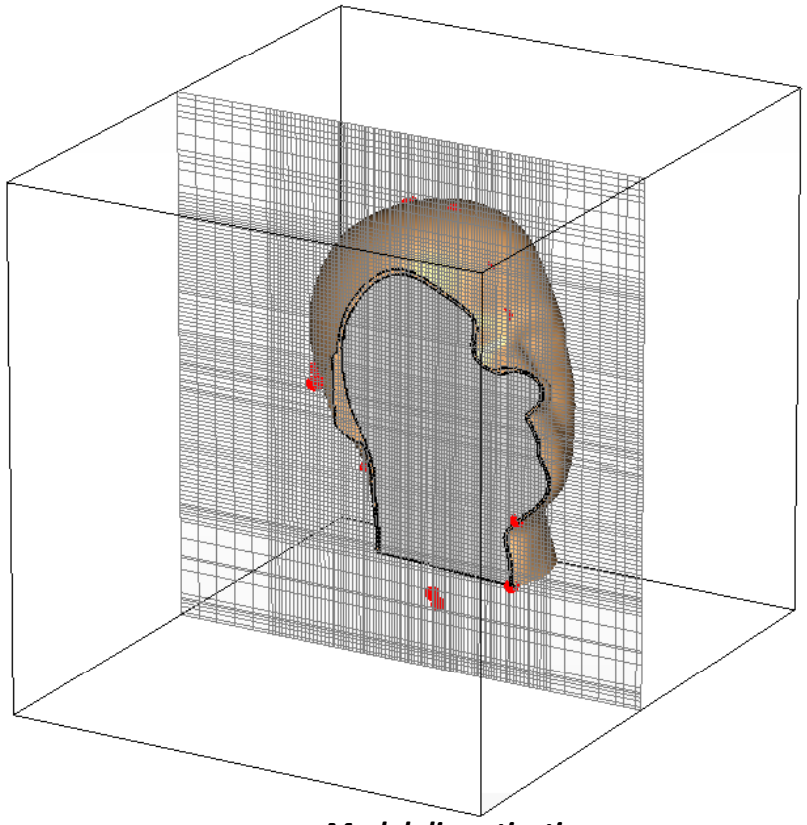

Model discretization

Pre-conditions before start of simulation

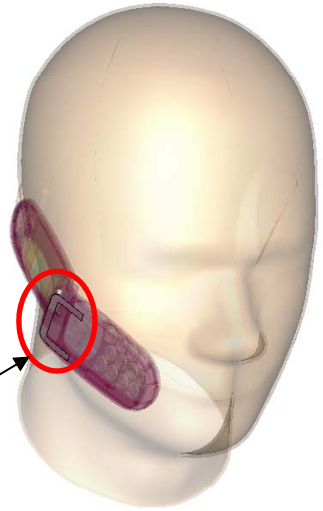

Dispersive material for head phantom

Frequency	Re($\tilde{\varepsilon}$)	Im ($\tilde{\varepsilon}$)
0.9GHz	41.5	17.98 (0.9S/m)
1.8GHz	40	13.98 (1.4S/m)

Define labeling

Choose the power loss density at the interested frequency

Define averaging mass density or point SAR

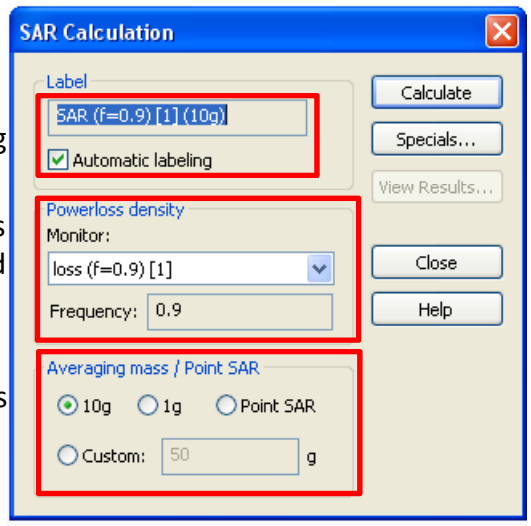

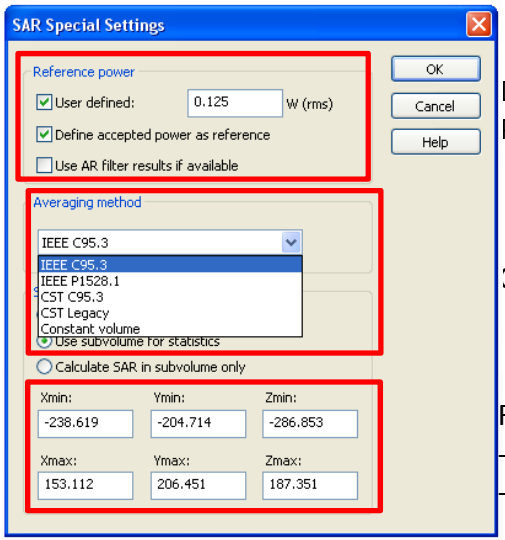

Define reference power, Port input or accepted power

Choose averaging method

Restrict volume for:
- maximum search and statistics
- reduced computational effort

SAR VISUALIZATION

2D or 3D plot including information about position of the maximum

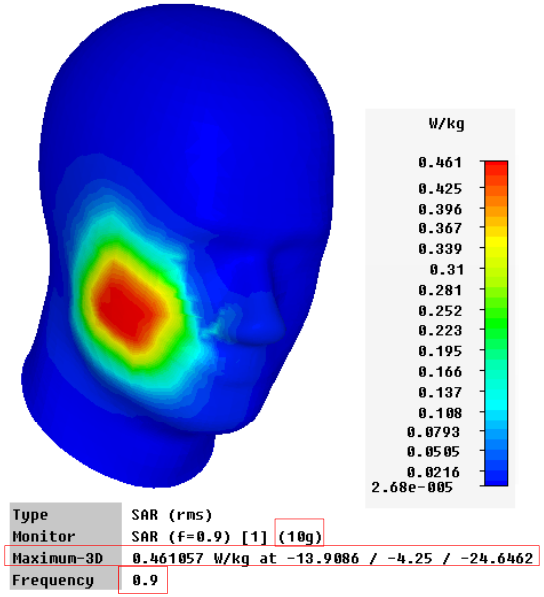

Type	SAR (rms)
Monitor	SAR (f=0.9) [1] (10g)
Maximum-3D	0.461057 W/kg at -13.9086 / -4.25 / -24.6462
Frequency	0.9

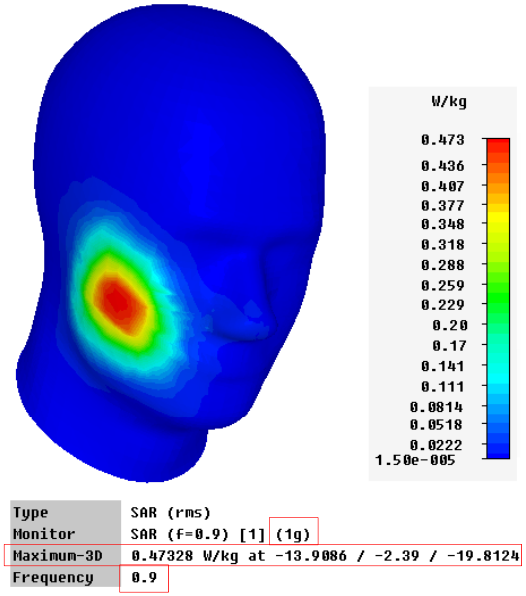

Type	SAR (rms)
Monitor	SAR (f=0.9) [1] (1g)
Maximum-3D	0.47328 W/kg at -13.9086 / -2.39 / -19.8124
Frequency	0.9

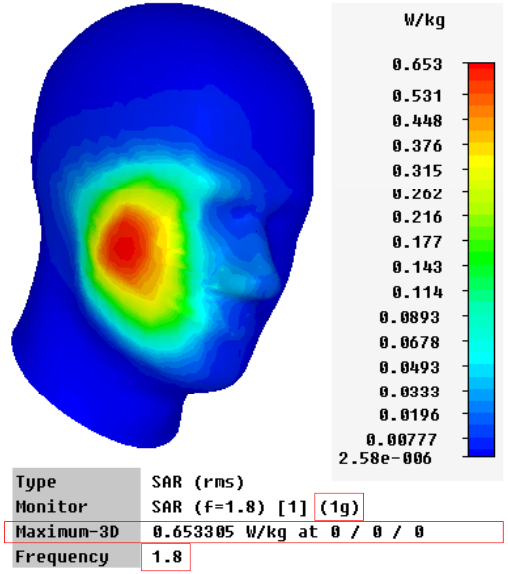

Type	SAR (rms)
Monitor	SAR (f=1.8) [1] (1g)
Maximum-3D	0.653305 W/kg at 0 / 0 / 0
Frequency	1.8

$$P_{\substack{antenna\\input}} = 1W$$

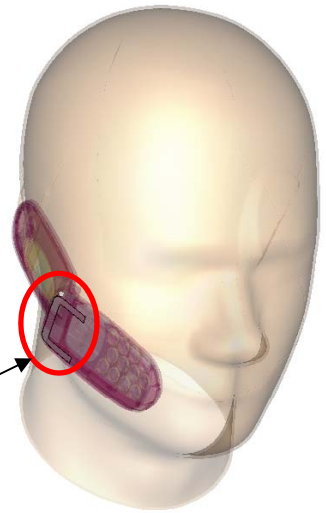

Planar Inverted F Antenna

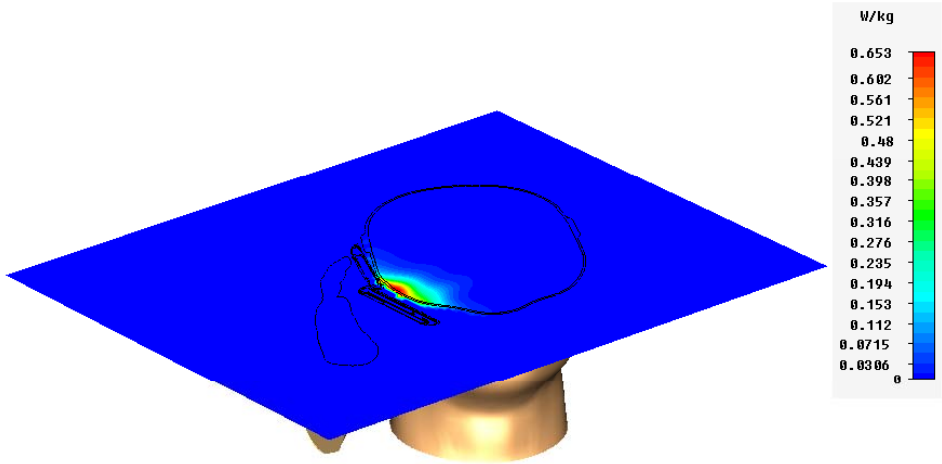

Type	SAR (rms)
Monitor	SAR (f=1.8) [1] (1g)
Plane at y	0.86821
Maximum-2D	0.653309 W/kg at -26.4808 / 2.19738 / -21.3366
Frequency	1.8

SAR RESULTS

General information

Statistics for total volume (head + hand)

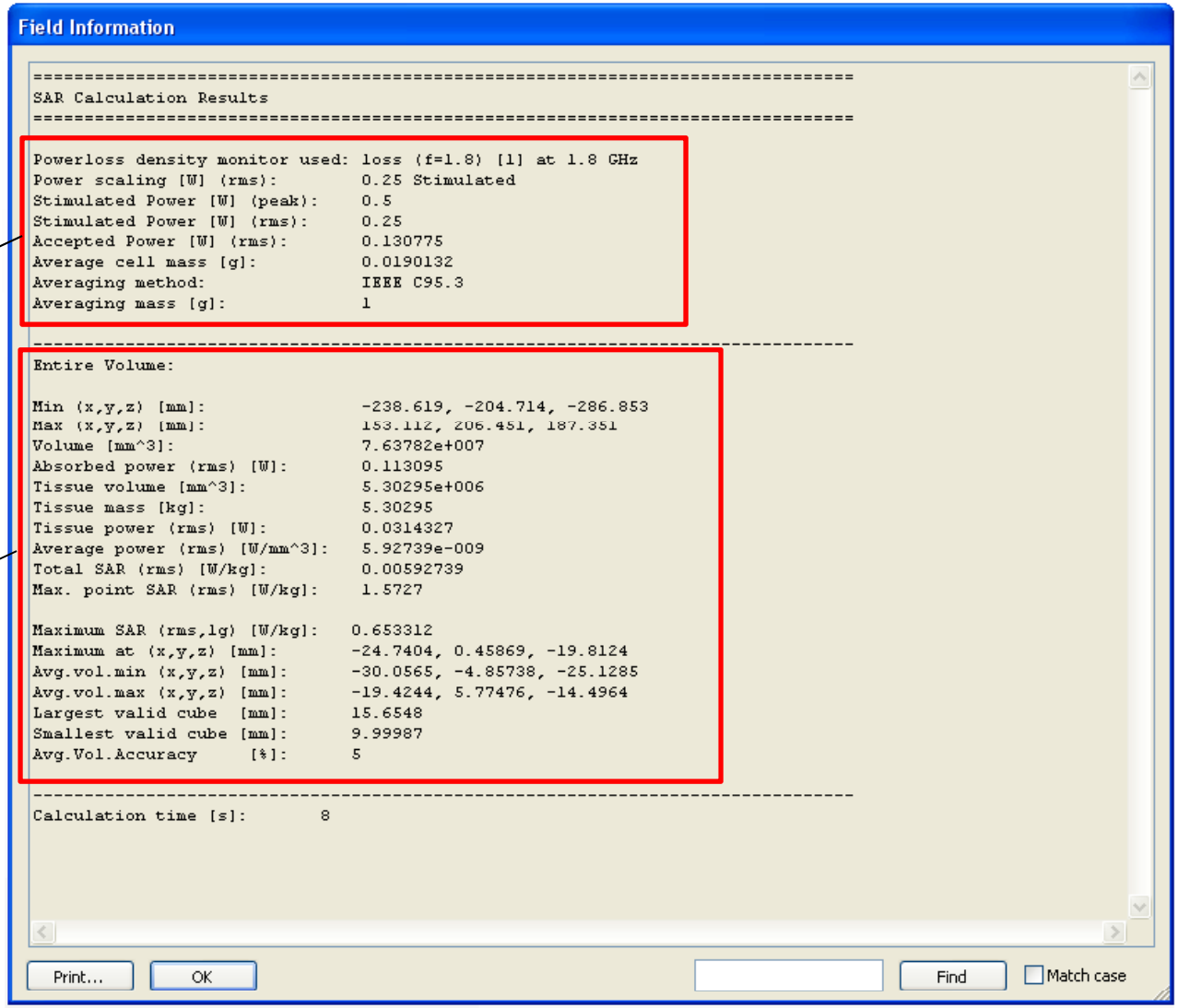

SAR IN A HUMAN HEAD USING RF-COIL AT 11.7T (500MHz)

- In ultra-high field (>8T) MRI systems, the RF coil is an essential element to provide a higher imaging quality at higher proton resonance frequencies (Larmor frequencies) with a reasonable B1-field homogeneity in the imaging area, low SAR in the biological tissues and a good signal to noise ratio (SNR).
- As frequencies increase, the wavelength shortens (60 cm in the vacuum and 8.5 cm inside the head at 500MHz), and becomes comparable to the electrical dimensions of the head/body and the RF coil. RF fields interact more strongly with human tissues and wave behavior of the B1-field should affect strongly its homogeneity inside the highly permittive and lossy tissues.
- While B1 inhomogeneities cause non uniform intensity distribution in MR images, the RF electric field counterpart, potentially inhomogeneous too, should expose biological tissues to an excessive RF power deposition with induced local heating.
- Numerical codes offer a very practical tool to investigate the distributions of the magnetic field and the maximum of local SAR values for various kind of coils. They allow the calculations of expected SARs for MRI typical pulse sequences in accordance to guidelines.

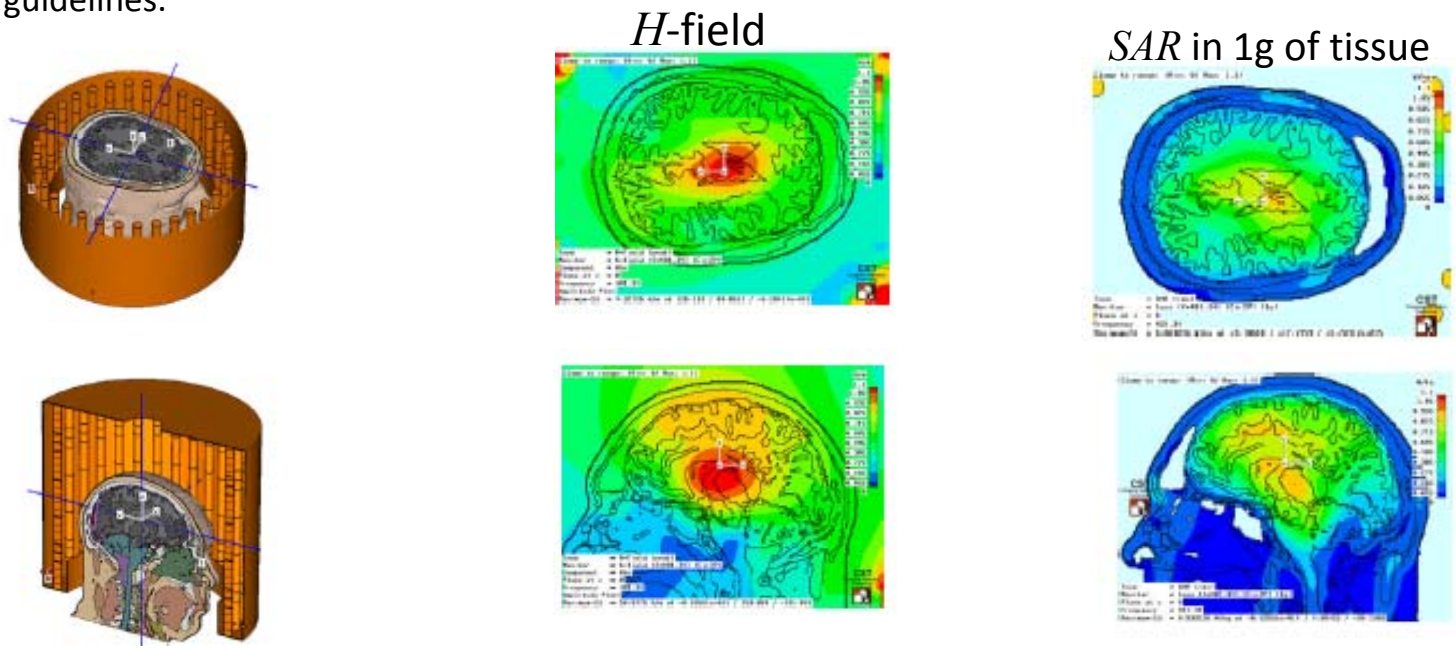

SAR_{max} is 1.14W/kg localized in the center of the brain

References

1. D. Andreuccetti, M. Bini, A. Checcucci, A. Ignesti, L. Millanta, R. Olmi, N. Rubino, “Protezione dai campi elettromagnetici non ionizzanti”, 3a Edizione, *IROE “Nello Carrara” CNR*, Firenze 2001.
2. J. Lin, A.W. Guy, and C.C. Johnson, “Power deposition in a spherical model of a man exposed to 1-20 MHz electromagnetic fields”, *IEEE Trans. on MTT*, December 1973.
3. P.W. Barber, OM.P. Gandhi, M.J. Hagmann, I. Chatterjee, “Electromagnetic Absorption in a multi-layered model of man”, *IEEE Trans on Biomed. Eng.*, vol. BME-26, no. 7, July 1979.
4. C.C. Johnson, C.H. Durney, H. Massoudi, “Long-wavelength electromagnetic power absorption in prolate spheroidal models of man and animals”, *IEEE Trans. On MTT*, vol. MTT-23, no.9, pp. 739-747, September 1975.
5. H. Massoudi, C.H. Durney, C.C. Johnson, “Long-wavelength electromagnetic power absorption in ellipsoidal models of man and animals ”, *IEEE Trans. On MTT*, vol. MTT-25, no.1, pp. 47-52, January 1977.
6. M. Hagmann, OM. P. Gandhi, C.H. Durney, “Numerical calculation of electromagnetic energy deposition for a realistic model of man”, *IEEE Trans. On MTT*, vol. MTT-27, no. 9, September 1979.
7. H. Massoudi, “A geometrical optics and an exact solution for internal fields and energy absorption by a cylindrical model of man irradiated by an electromagnetic plane wave”, *Radio Science*, vol.14, no. 6S, pp. 35-42, November-December 1979.
8. C.H. Durney, “Electromagnetic dosimetry for models of humans and animals - A review of theoretical and numerical techniques”, *IEEE Proceedings*, vol. 68, no. 1, pp. 33-40, January 1980.
9. ww.cst.com